

Contents lists available at ScienceDirect

Geoderma

journal homepage: www.elsevier.com/locate/geoderma



Does soil erosion rejuvenate the soil phosphorus inventory?

Andre Eger^{a,*}, Kyungsoo Yoo^b, Peter C. Almond^c, Gustavo Boitt^c, Isaac J. Larsen^d, Leo M. Condron^c, Xiang Wang^b, Simon M. Mudd^e

- ^a Landcare Research, Department Soil and Landscapes, Gerald St, Lincoln 7608, New Zealand
- ^b University of Minnesota, Department of Soil, Water, and Climate, 439 Borlaug Hall, 1991 Upper Buford Circle, St. Paul, MN 55108-6028, USA
- ^c Lincoln University, Department of Soil and Physical Sciences, PO Box 85084, Lincoln 7647, New Zealand
- d University of Massachusetts, Department of Geosciences, 627 North Pleasant Street, 233 Morrill Science Center, Amherst, MA 01003-9297, USA
- ^e University of Edinburgh, School of GeoSciences, Geography Building, Drummond Street, Edinburgh EH8 9XP, UK



ARTICLE INFO

Handling Editor: M. Vepraskas
Keywords:
Soil phosphorus
Phosphorus fractionation
Soil residence time
Soil age
Soil erosion
Hillslopes

Soil chronosequences

Soil parent material

ABSTRACT

Phosphorus (P) is an essential nutrient for life. Deficits in soil P reduce primary production and alter biodiversity. A soil P paradigm based on studies of soils that form on flat topography, where erosion rates are minimal, indicates P is supplied to soil mainly as apatite from the underlying parent material and over time is lost via weathering or transformed into labile and less-bioavailable secondary forms. However, little is systematically known about P transformation and bioavailability on eroding hillslopes, which make up the majority of Earth's surface. By linking soil residence time to P fractions in soils and parent material, we show that the traditional concept of P transformation as a function of time has limited applicability to hillslope soils of the western Southern Alps (New Zealand) and Northern Sierra Nevada (USA). Instead, the P inventory of eroding soils at these sites is dominated by secondary P forms across a range of soil residence times, an observation consistent with previously published soil P data. The findings for hillslope soils contrast with those from minimally eroding soils used in chronosequence studies, where the soil P paradigm originated, because chronosequences are often located on landforms where parent materials are less chemically altered and therefore richer in apatite P compared to soils on hillslopes, which are generally underlain by pre-weathered parent material (e.g., saprolite). The geomorphic history of the soil parent material is the likely cause of soil P inventory differences for eroding hillslope soils versus geomorphically stable chronosequence soils. Additionally, plants and dust seem to play an important role in vertically redistributing P in hillslope soils. Given the dominance of secondary soil P in hillslope soils, limits to ecosystem development caused by an undersupply of bio-available P may be more relevant to hillslopes than previously thought.

1. Introduction

Phosphorus (P) is an essential element for all life on Earth through its role in forming ATP and as a structural component of DNA (Nelson et al., 2008). Consequently, the P cycle in terrestrial and marine environments has been studied extensively (Filippelli, 2002; Paytan and McLaughlin, 2007; Turner and Condron, 2013; Walker and Syers, 1976). Ecological research has shown that P fertility of terrestrial ecosystems is strongly linked to the weathering trajectory of soils with time: on geomorphically stable landforms, increasingly chemically altered soils lead to a declining pool of plant-available P, which can cause a decline of primary production and biomass, and strongly influence species and functional diversity (Crews et al., 1995; Eger et al., 2013b; Peltzer et al., 2010; Zemunik et al., 2015). The depletion of plant-available P, however, is not simply a result of P weathering loss but also

due to intensive biochemical transformations and recycling (Frossard et al., 2000).

Our current understanding of long-term P transformations is largely based on soil chronosequence studies; a study concept that takes advantage of a set of landforms that formed at different but known times in the past that have been minimally rejuvenated by erosion or deposition. In this framework, all other soil forming factors since cessation of erosion or deposition are assumed to have been similar between sites, allowing for isolation of the influence of time on soil development. Synthesising multiple soil chronosequences in New Zealand, Walker and Syers (1976) established the seminal soil P development concept: with increasing time, bio-available P declines as a result of leaching and the transformation of primary, rock-derived apatite P into less directly bio-available P forms such as organic P and P adsorbed to or occluded into secondary oxides. Whereas apatite P can be made directly bio-

E-mail address: egera@landcareresearch.co.nz (A. Eger).

^{*} Corresponding author.

available as PO₄³⁻ through mineral dissolution in an acidic soil environment, the physically occluded P fraction, in particular, comprises P forms that are highly stabilized (Smeck, 1985) and hence not readily accessible by biota as a result of physical protection in mineral structures (primary or secondary silicate minerals, oxides, oxyhydroxides), organic matter and soil micro-aggregates (Blake et al., 2003; Guo and Yost, 1998). The Walker and Syers paradigm of P development has been found to be generally valid for a range of soils in different climatic and lithologic settings (Crews et al., 1995; Eger et al., 2011; Selmants and Hart, 2010; Turner and Laliberté, 2015).

However, the nominally non-eroding setting of a chronosequence is a special case, as most of Earth's surface undergoes either net erosion (Larsen et al., 2014b) or deposition, Hillslopes are predominantly erosional landforms, where gravity and physical disturbances facilitated by water or bioturbation drive the downslope movement of soil, which is then delivered to fluvial systems or deposited on convergent sections of slopes or at slope-valley transitions. As mass is physically and chemically lost from a soil profile on an eroding hillslope, soil cover is maintained over time by the counterbalancing process of soil production (Gilbert, 1877; Heimsath et al., 1997), the conversion of parent material to soil. Soil production is regarded as a natural rejuvenator of soil nutrients by the replacement of weathered, nutrient-poor material with unweathered substrate (Amundson et al., 2015; Porder and Hilley, 2011; Porder et al., 2007b; Vitousek et al., 2003). The 'fertilisation' through soil production on slopes could be especially significant for soil P because in most terrestrial settings P is supplied to the biogeochemical cycle by weathering of the P-bearing mineral apatite and hence is delivered to the base of the soil by the parent material, unless there are external sources of P, such as atmospheric input. Dust has a major impact on soil P budgets in sufficiently P-depleted soils and/or where dust deposition rates are high (e.g., Chadwick et al., 1999; Eger et al., 2013a). Atmospheric input may even play an important role in P cycling at younger stages of ecosystem development in some locations (Arvin et al., 2017; Boyle et al., 2013).

The role of hillslope topography and soil erosion processes need to be considered when evaluating soil P pools and fractionation as it will affect the time soil material is residing on the slope before removal by chemical or physical processes (Agbenin and Tiessen, 1994; Amundson et al., 2015; Porder and Hilley, 2011; Porder et al., 2007b; Vitousek et al., 2003). For example, in Hawaii lower proportions of occluded P but more organic P were found on a hillslope in comparison to the geomorphically stable shield surface, indicating rejuvenation via slope dynamics (erosion and deposition) (Vitousek et al., 2003). However, no clear trends of P fractionation existed across the hillslope itself, from the shoulder (younger soils) to the toeslope (older soils). P fractionation data from ridge-slope-valley transects in Puerto Rico demonstrated the dominant control on the spatial distribution of more labile P forms was topography; labile P was lowest on the ridge and generally increased downslope toward the valley (Mage and Porder, 2013). In contrast, parent material was the main control on occluded and total P, with the highest values in the valleys, and apatite P (< 5% of total P in all soils) was unrelated to either topography or parent material (Mage and Porder, 2013). Selected soil P fractions (total P, apatite P, labile P and occluded P at 0-20 cm depth) on ridgetops in Puerto Rico were not significantly controlled by erosion rates or soil residence time, however, erosion rates and residence times varied little between sites (McClintock et al., 2015). Data from slope transects in Brazil showed that young upper slope soils (Entisols) have higher apatite P and lower labile P concentrations than Inceptisols in mid and lower slope positions (Agbenin and Tiessen, 1994). Differences in relative soil residence times induced by erosion were deemed the likely reason for the behaviour of apatite P. With only the study from Brazil adhering to the Pdevelopment concept derived from chronosequences, the relationship between P fractions and the relative soil age on slopes is less clear.

The divergence in P fractionation on eroding slopes relative to what is predicted from chronosequence studies highlights the need to

reconcile the apparently different behaviour of P observed in different topographic settings. We suggest that comparing these findings in the context of soil P evolution as proposed by Walker and Syers (1976) is the most promising approach. Amundson et al. (2015) proposed a unifying concept in which temporal shifts from N to P nutrient limitation in terrestrial ecosystems are related to the continuum of residence times of minerals within the soil. The concept of Amundson et al. (2015) builds on new appreciation of tectonic uplift as a driver of erosion and thus P supply in the otherwise P-depleted tropical soils (Porder et al., 2007b). Uplift is typically associated with tectonic plate margins and a major control of erosion rates that are inversely related to soil residence times. Soil residence time in these studies is defined as the length of time that is required for soil material to be removed by erosion and replaced by soil production, and during which soil particles experience physical and biogeochemical conditions at the top of the weathering profile (Almond et al., 2007; Dere et al., 2013; McClintock et al., 2015). Compared to chronosequences developed in flat landforms, Amundson et al. (2015) suggested that residence times for most hillslope soils in temperate climates give rise to neither N nor P limitation. In other words, soils on eroding hillslopes are not too young to have N limitation or too old to be depleted in mineral P.

Whether eroding hillslope soils indeed occupy an optimal residence time window with respect to P limitation remains to be tested. There are few data that directly link individual P fractions to absolute soil residence times (McClintock et al., 2015). Additionally, previous studies of soil P on eroding hillslopes are largely limited to tropical landscapes (Abekoe and Tiessen, 1998; Agbenin and Tiessen, 1994; Araújo et al., 2004; Mage and Porder, 2013; McClintock et al., 2015; Porder and Hilley, 2011; Porder et al., 2007b; Vitousek et al., 2003). In these actively eroding tropical systems, deep chemical alteration of bedrock causes soils to be depleted in apatite P, which provides the first indication that the optimal window hypothesis may not be applicable globally. However, the applicability of these studies from tropical landscapes to extra-tropical regions may also be limited. In contrast to temperate climate regions, in the tropics, deep and more completely weathered profiles prevail, mineralisation rates of organic matter are higher, low-reactivity clays and pedogenic oxide/hydroxides increasingly dominate the residual soils, and the legacy of glacial/periglacial conditions during the Pleistocene is largely absent.

Here we present new P fractionation data quantitatively linked to hillslope soil residence times across two gradients of erosion rates in temperate ecosystems and compare them to published results regarding patterns and rates of P transformation. We initially hypothesised, based on the proposal by Amundson et al. (2015), that higher soil production and erosion rates and hence shorter residence times result in high total soil P concentrations and high proportions of primary mineral P as expected for immature soils, whereas lower erosion rates and longer residence times result in low total soil P due to the intensive weathering of older soil particles, and a high proportion of secondary P forms as expected in more mature soils. However, our data do not support this hypothesis and instead, somewhat distinct from the conceptual framework laid out in Walker and Syers (1976), highlight the significance of weathering below the base of the soil in temperate climates, biological uptake of P and potential dust accretion.

2. Methods

2.1. Definition of mean soil particle age, residence time, turnover time and comparison with soil age

We first require a consistent framework for the measure of time for our soils. As we will show, soil residence time and soil age provide consistent temporal references to which soil P dynamics from geomorphically active and stable landscapes can be compared. We conceptualize that the mass balance of a hillslope soil (Fig. 1) is largely determined by the difference between the mass losses via physical and

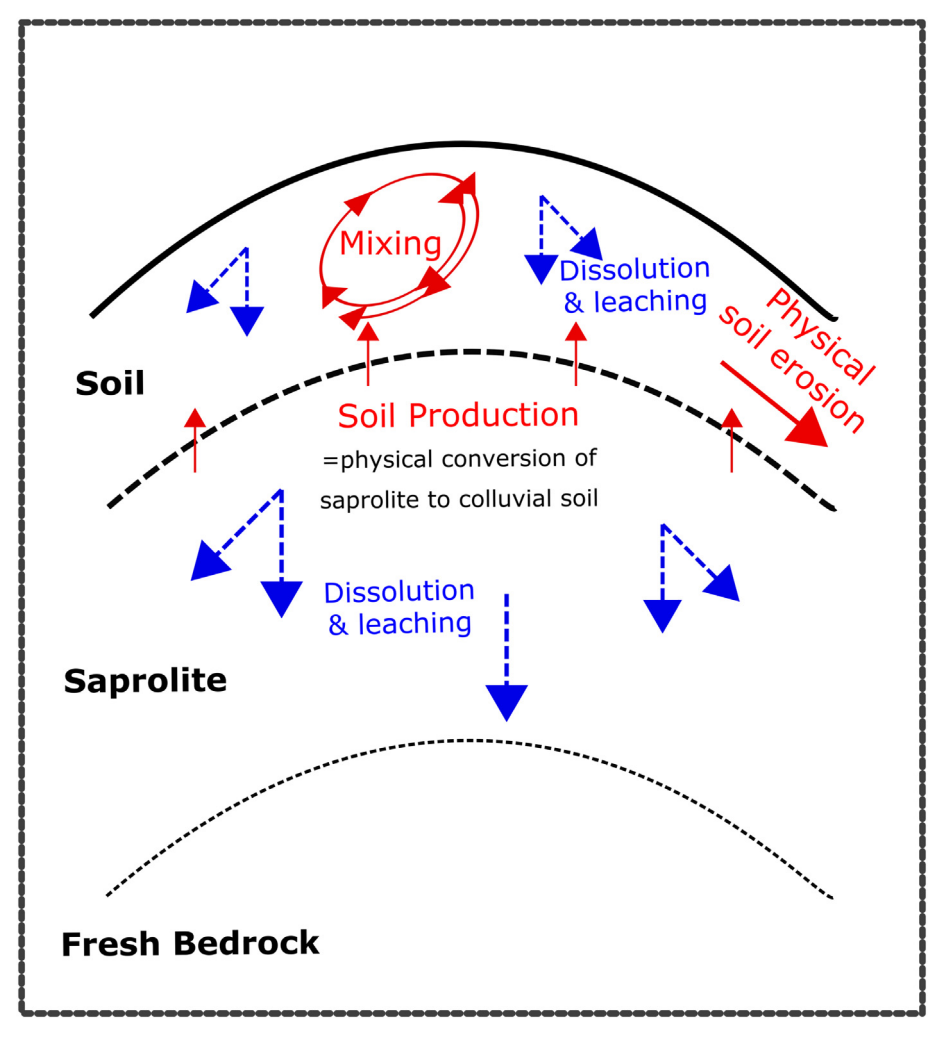


Fig. 1. Simplified conceptual model of hillslope processes affecting soils at steady-state soil thickness. See text for detailed discussion.

chemical erosion and mass input via soil production; our conceptualization assumes aeolian inputs are negligible. In this simplified view, a hillslope soil is defined as a part of a weathering profile that has been not only chemically weathered but also physically disturbed and mixed. In contrast, the lower part of the weathering profile is considered chemically weathered but physically undisturbed (i.e., saprolite). We assume soil mass removal via physical and chemical erosion is balanced by soil production, such that a steady-state is reached (Heimsath et al., 1997). Since our focus is on transformations and losses of P in hillslope soils (i.e., soil as the residual of the weathering process), we are concerned with the ages of the particles with respect to their initial incorporation within the soil, as exposure to weathering and leaching increases as a function of particle age. Hillslope soil particles have a distribution of age that is unknowable in all but the simplest case of steady state soil thickness, together with either complete mixing or plug flow (Mudd and Yoo, 2010) and the absence of chemical weathering. Hence, pragmatically, we seek only a metric to rank soils according their exposure to weathering. Under aforementioned simplifying conditions, mean particle age of the soil (ψ) , mean soil residence time (χ , average age of particles leaving the soil) and soil turnover time (φ , the length of time that it takes for a soil particle to be completely depleted by the outgoing flux) are equal (Almond et al., 2007; Mudd and Yoo, 2010; Yoo and Mudd, 2008). We adopt the mean particle age, and, assuming perfect mixing and steady state in the absence of chemical weathering, we estimate it by the soil turnover time. Soil turnover time is calculated as the ratio of the mass of the soil and the outgoing mass flux from that soil (Mudd and Yoo, 2010). Assuming

steady state, the outgoing mass flux (erosion) equals the rate of conversion of parent material to soil (i.e., soil production rate) as determined by cosmogenic nuclide measurements at each of our sites (see below) corrected for chemical mass loss.

$$\psi = \varphi = \chi = \frac{[Zr]_s}{[Zr]_r} \frac{\rho_s h}{\rho_r D} \tag{1}$$

where ψ is mean particle age, φ residence time and χ is turnover time (T). [Zr] represents the mass concentration of the immobile element zirconium (MM⁻¹), ρ is bulk density (ML⁻³), h is soil thickness (L), D is soil production/erosion rate (LT^{-1}), and subscripts s and r indicate soil and parent material, respectively. The term [Zr]_s/[Zr]_r converts the soil erosion rate, which includes a chemical weathering component, into a physical erosion rate (e.g., Riebe et al., 2003). Since soil thickness and soil production rate units are given in length, the inclusion of ρ_s/ρ_r accounts for the dilation between parent material and soil. Here [Zr]_s/ [Zr]_r is typically larger than 1 because of Zr enrichment in soils as a result of leaching of other more soluble elements. In contrast, the bulk density ratio between soils and the parent material is typically < 1, contributing to cancelling the effect of Zr enrichment in soils. Thus we further simplify our soil particle age metric to h/D, similar to other studies (e.g., Amundson et al., 2015; Porder et al., 2007b). In the literature, mean soil particle age, mean soil residence time, or soil turnover time have been used interchangeably or authors simply referred to soil residence time without strict definitions based on reservoir theory (e.g., Almond et al., 2007; Amundson et al., 2015; Green et al., 2006; Porder and Hilley, 2011). We follow this convention and use the term

soil residence time instead of the mean particle age or turnover time.

While an approximate steady state is a useful concept for investigating eroding soils, soils developing on geomorphically stable landforms are only minimally affected by physical erosion. Still, a mean age of soil mineral particles can be defined (Yoo and Mudd, 2008). A soil consists of mineral particles that have a range of time lengths (i.e., ages) since their physical incorporation into the soil from the underlying parent materials. The maximum age of mineral grains cannot be older than the age of the soil, however. Soil age is defined as time length since cessation of erosion or deposition. Additionally, in noneroding chronosequences, soils become increasingly thicker with time as chemically more inert soil material residually accumulates, which slows the downward propagation of soil development into the parent material (Lebedeva et al., 2010), and hence the rate of incorporation of nutrient-replenishing parent material (Yoo and Mudd, 2008). Thus, the number of mineral grains introduced to the soil from the underlying parent material exponentially decreases over time. As a consequence, it is expected that the mean age of the mineral particles is less than soil age, but the distribution of individual mineral grains' ages is skewed toward the early phase of soil formation. Thus, the mean age of mineral grains in a soil is proportional to the soil age (Yoo and Mudd, 2008).

2.2. Study site and field sampling

The P data come from two temperate locations that differ substantially in rainfall and soil production/erosion rates. Soil thicknesses, soil production/erosion rates, and calculated soil residence times (Eq. (1)) for each soil are reported in Tables 1 and 2. Soil thicknesses and soil production/erosion rates were reported previously and the methods and discussion concerning these data, and the range of parameters are described by Larsen et al. (2014a) for the Western Southern Alps (WSA)

sites, and Hurst et al. (2012) and Yoo et al. (2011) for the Feather River (FR) sites. Soil residence times at FR sites were also reported in Wang et al. (2018).

The first study area is located in the western Southern Alps (WSA) of New Zealand at the collisional boundary of the Australian and Pacific Plates (Fig. 2), resulting in up to 10 mm y⁻¹ tectonic uplift (Little et al., 2005; Tippett and Kamp, 1993). Soil parent material is schist derived from a greywacke protolith. The Southern Alps form an orographic barrier against the prevailing westerly airstream resulting in a mean annual precipitation of 10.391 mm (1979-2015, maximum Dec 1099 mm, minimum July 643 mm), with a mean annual temperature of 5.5 °C (NIWA, 2016: Tonkin and Basher, 2001) at ~900 m asl. The natural vegetation cover is a podocarp-hardwood forest and subalpine, dense scrub/low tree communities (Wardle, 1977). Topography is heavily dissected by a dense drainage network of steep, V-shaped valleys including waterfalls, gorges, and narrow ridge lines (Whitehouse, 1988). Landslides are frequent as a result of earthquakes and high rainfall (Hilton et al., 2008; Hovius et al., 1997; Korup et al., 2004), but return intervals are long enough to allow the formation of thin soil and regolith cover at any point on the landscape between failures (Larsen et al., 2014a; Whitehouse, 1988).

The soil production/erosion rates in the WSA (Table 1) are amongst the highest in the world (Larsen et al., 2014a) and the soils are weakly developed Entisols or Inceptisols (Soil Survey Staff, 2014). All individual soil sampling sites were located on the main ridges or in local, meter-scale convexities on smaller divides emanating from the main ridges to avoid effects from landsliding. As such the site selection aimed at fulfilling the steady state assumption required by the in-situ cosmogenic nuclide method to yield reliable soil production rates at each site. We do not necessarily expect these sites to be representative of the average soil thickness in each of the WSA catchments. Local slope at the soil sites ranged between 24° to 50°.

Table 1Soil data for the WSA sites.

Soil sampling sites	Soil taxonomy	Mineralogical	Textural	Soil depth	Altitude	Soil residence time	Total erosion rate ^a	pН	P _{total} mg kg ⁻¹	P _{org}	P _{Fe/Al}	P _{apatite}	P _{occ}
		zone	zone	cm	m asl	years	mm y ⁻¹	-					
Fox 1	n.d.	Oligoclase amphibolite	TZ4	32	932	1391 ± 121	0.23 ± 0.02	3.2	429	163	173	25	67
Fox 2	n.d.	Oligoclase amphibolite	TZ4	20	942	1818 ± 165	0.11 ± 0.01	3.7	304	59	116	10	119
Alex Knob 2	n.d.	Oligoclase amphibolite	TZ4	41	846	2563 ± 160	0.16 ± 0.01	3.5	334	148	82	23	80
Alex Knob 3	n.d.	Oligoclase amphibolite	TZ4	15	947	833 ± 46	$0.18~\pm~0.01$	4.6	663	8	230	70	355
Alex Knob 4	Lithic udorthent	Oligoclase amphibolite	TZ4	30	836	$2143~\pm~153$	$0.14~\pm~0.01$	3.5	433	110	136	33	154
Karangarua 1	Humic lithic dystrudept	Garnet greenschist	TZ4	40	1030	$1333~\pm~89$	$0.30~\pm~0.02$	4.5	419	56	146	70	147
Karangarua 2	Lithic udorthent	Garnet greenschist	TZ4	21	1082	1313 ± 82	0.16 ± 0.01	3.6	591	139	155	57	240
Karangarua 3	Lithic udorthent	Garnet greenschist	TZ4	15	1112	1364 ± 124	0.11 ± 0.01	4.8	476	46	191	46	194
Karangarua 4	Humic lithic dystrudept	Garnet greenschist	TZ4	21	959	553 ± 44	0.38 ± 0.03	4.0	427	50	143	46	188
Karangarua 5	Lithic udorthent	Garnet greenschist	TZ4	10	961	323 ± 21	0.31 ± 0.02	3.5	379	132	70	37	140
Rapid Creek 1	Lithic dystrudept	Garnet amphibolite	TZ4	40	966	1176 ± 104	0.34 ± 0.03	4.4	749	24	257	73	395
Rapid Creek 2	Lithic dystrudept	Garnet amphibolite	TZ4	30	897	405 ± 33	0.74 ± 0.06	3.5	484	141	136	43	164
Rapid Creek 3	Humic lithic dystrudept	Garnet amphibolite	TZ4	16	856	160 ± 13	1.00 ± 0.08	3.7	494	49	191	40	213
Rapid Creek 4	Lithic udorthent	Garnet amphibolite	TZ4	12	946	49 ± 10	2.47 ± 0.51	4.4	963	56	252	140	514
Rapid Creek 5	Lithic udorthent	Garnet amphibolite	TZ4	15	832	142 ± 11	1.06 ± 0.08	3.4	934	485	134	85	229
Gunn Ridge 1	Lithic dystrudept	Chlorite greenschist	TZ3	24	866	462 ± 36	0.52 ± 0.04	3.6	432	159	89	56	128
Gunn Ridge 2	Lithic dystrudept	Chlorite greenschist	TZ3	25	832	694 ± 58	0.36 ± 0.03	3.4	375	172	53	42	107
Gunn Ridge 3	Lithic dystrudept	Chlorite greenschist	TZ3	29	856	744 ± 57	0.39 ± 0.03	3.7	557	89	145	50	273
Gunn Ridge 4	Lithic endoaquept	Chlorite greenschist	TZ3	39	953	2053 ± 216	0.19 ± 0.02	3.5	411	110	80	26	196
Gunn Ridge 5	Humic lithic dystrudept	Chlorite greenschist	TZ3	30	910	1154 ± 89	0.26 ± 0.02	3.6	508	137	83	88	199
Gunn Ridge 6	Lithic dystrudept	Chlorite greenschist	TZ3	27	838	730 ± 59	0.37 ± 0.03	3.5	399	292	55	24	28
Gunn Ridge 7	Lithic dystrudept	Chlorite greenschist	TZ3	34	555	1308 ± 101	0.26 ± 0.02	3.6	410	177	61	24	148

^a Larsen et al. (2014a).

Table 2
Soil and saprolite data for the FR sites. The detailed and simplified P fractionations are shown. Note the residence time for BRC and POMD soils. No absolute residence time was calculated for the intermediate site.

Site	Sample depth	Soil horizon	pН	Pi _{NH4Cl}	Pi _{bic}	Po_{bic}	Pi _{OH} _I	Po _{OH} _I	Pi _{HCl}	Pi _{OH} _II	Po _{OH} _II	P _{residual}	P _{total}	P _{org}	P _{Fe/Al}	P _{apatite}	P _{occ}	
	cm		(water)	mg kg ⁻¹	$mg kg^{-1}$									mg kg ⁻¹				
Soil erosion rate 250 mm ⁻¹ ; 60 cm soil depth; soil residence time: 2400 y																		
BRC0	0–6	Α	6.9	0.4	27.3	13.2	153.9	159.8	14.0	60.3	23.7	106.0	558.6	197	154	14	166	
BRC0	6–10	A/B	6.5	0.1	5.0	9.9	64.3	73.8	6.8	29.9	25.1	99.9	314.8	109	64	7	130	
BRC0	10-20	Bw1	n.d.	0.1	2.7	10.7	44.4	80.9	4.9	24.5	28.9	110.5	307.5	120	44	5	135	
BRC0	20-30	Bw1	6.3	0.1	1.9	9.8	25.4	92.2	4.7	24.3	31.1	107.1	296.5	133	25	5	131	
BRC0	30–40	Bw1	n.d.	0.1	2.5	8.6	30.9	96.0	4.4	26.2	30.7	125.5	324.9	135	31	4	152	
BRC0	40–50	Bw2	n.d.	0.1	1.9	8.7	18.7	82.2	2.3	18.2	25.8	96.9	254.8	117	19	2	115	
BRC0	50–60	Bw2	n.d.	0.1	2.4	12.1	20.5	85.5	2.2	16.5	24.1	107.2	270.5	122	21	2	124	
BRC0	60–90	Cr	6.0	0.1	2.3	7.0	16.2	73.4	2.0	14.6	19.3	101.8	236.8	100	16	2	116	
BRC0	90–100	Cr	n.d.	0.1	5.7	6.6	40.9	78.0	3.5	22.9	26.3	89.2	273.1	111	41	4	112	
	on rate 250 mm	⁻¹ ; 44 cm soil d	epth; soil 1	esidence t	ime: 18	•												
BRC3	0–1	A	6.4	1.11	44.4	19.4	123.5	94.3	16.7	32.5	27.6	87.0	446.6	141	124	17	120	
BRC3	1–15	AB	6.0	0.11	4.6	12.5	52.8	84.3	7.8	24.4	32.8	92.3	311.6	130	53	8	117	
BRC3	15–44	Bw	6.5	0.07	0.7	11.1	32.7	75.3	6.4	20.9	27.9	95.9	271.1	114	33	6	117	
BRC3	44–72	Cr1	5.8	0.04	5.4	10.5	41.1	71.2	7.7	19.2	26.6	80.1	261.9	108	41	8	99	
Soil erosion rate between 35.7 and $250 \mathrm{mm}^{-1}$; 79 cm soil depth																		
FTA1	0–8	Α	6.8	0.6	29.6	5.7	181.4	124.8	30.9	73.3	24.7	127.3	598.4	155	181	31	201	
FTA1	8–16	AB	5.6	0.3	8.7	18.9	78.2	62.7	6.7	31.8	29.9	122.2	359.3	111	78	7	154	
FTA1	16–24	AB	n.d.	0.1	3.3	23.8	58.1	76.9	4.0	25.3	30.0	115.1	336.6	131	58	4	140	
FTA1	24-34	AB	n.d.	0.1	2.6	12.4	48.7	77.2	2.8	22.6	27.3	116.1	309.7	117	49	3	139	
FTA1	34-44	Bw1	n.d.	0.1	2.4	9.9	32.7	83.3	1.9	17.2	24.7	102.3	274.5	118	33	2	120	
FTA1	44–55	Bw1	n.d.	0.1	2.8	10.1	25.5	75.2	1.6	17.1	23.6	104.9	260.9	109	26	2	122	
FTA1	55–67	Bw2	5.8	0.1	2.8	9.3	28.3	70.9	1.6	16.2	23.9	98.6	251.7	104	28	2	115	
FTA1	67–79	Bw2	n.d.	0.1	3.4	13.2	64.6	60.7	1.7	19.2	31.8	109.0	303.6	106	65	2	128	
FTA1	79–94	Cr	5.8	0.1	5.8	10.3	38.7	97.3	1.5	20.8	32.1	98.4	305.0	140	39	2	119	
FTA1	120–140	Cr	n.d.	0.1	4.9	9.1	28.7	71.3	1.4	19.0	16.3	103.3	254.1	97	29	1	122	
FTA1	152–163	Cr	n.d.	0.1	6.0	7.5	30.6	59.3	1.6	19.7	16.5	112.5	253.9	83	31	2	132	
Soil erosi	on rate between	35.7 and 250 m	ım ⁻¹ ; 63 c	m soil dep	th													
FTA8	0–8	A	6.1	0.43	39.6	17.9	159.0	128.1	14.7	41.4	34.6	105.5	541.2	181	159	15	147	
FTA8	8–13	A/B	5.6	0.11	8.8	14.8	61.7	117.1	7.7	23.6	31.6	104.3	369.6	163	62	8	128	
FTA8	13–19	A/B	n.d.	0.11	7.9	7.4	53.4	99.8	6.1	22.8	29.8	110.8	338.1	137	53	6	134	
FTA8	19–27	Bw1	n.d.	0.07	8.0	8.8	50.0	107.0	6.0	22.7	36.2	118.0	356.7	152	50	6	141	
FTA8	27–36	Bw1	5.7	0.07	4.1	7.3	49.3	83.6	4.5	19.1	30.5	101.1	299.8	122	49	5	120	
FTA8	36–45	Bw2	n.d.	0.11	3.9	7.8	36.7	79.6	5.8	19.1	28.7	104.1	286.0	116	37	6	123	
FTA8	45–54	Bw2	n.d.	0.07	2.5	8.0	36.7	94.8	4.1	20.6	27.1	117.9	311.7	130	37	4	138	
FTA8	54–63	Bw2	n.d.	0.07	1.2	11.0	31.8	63.3	4.0	18.7	21.4	111.6	263.1	96	32	4	130	
FTA8	63–90	Cr	6.4	0.11	5.7	1.8	27.0	39.3	9.5	17.4	12.0	94.6	207.4	53	27	9	112	
FTA8	90–120	Cr	n.d.	0.07	5.4	3.9	32.5	44.6	7.8	20.0	13.4	100.0	227.7	62	32	8	120	
FTA8	135–153	Cr	n.d.	0.11	2.8	3.1	22.7	29.0	3.4	17.3	11.7	91.6	181.7	44	23	3	109	
FTA8	165–174	Cr	n.d.	0.07	6.1	0.0	19.3	23.4	6.0	11.5	8.5	83.8	158.7	32	19	6	95 75	
FTA8 FTA8	183–188 190–202	Cr Cr	n.d. n.d.	0.07 0.07	3.4 5.6	3.4 1.4	20.1 17.1	34.1 30.3	8.1 5.6	11.8 12.2	9.2 7.9	63.3 78.0	153.5 158.3	47 40	20 17	8 6	75 90	
FTA8	207–213	Cr	n.d.	0.07	3.5	3.4	17.1	20.3	6.9	7.9	14.6	53.2	127.1	38	17	7	61	
							17.1	20.5	0.5	7.5	14.0	33.2	12/.1	30	1/	,	01	
	on rate 35.7 mm																	
POMD0	0–5	A	5.9	1.7		10.9	92.4	54.0	13.4	25.6	12.4	111.3	368.7	77	92	13	137	
POMD0	5–10	A B/A	5.0	0.3	7.9	14.6	36.8	68.1	4.5	15.7	14.1	113.8	275.8	97 75	37	4	129	
POMD0	10-20	B/A	n.d.	0.1	3.3	10.6	22.4	51.0	3.3	13.0	13.6	96.6	213.9	75 73	22	3	110	
POMDO	20–30	B/A	6.0	0.1	2.4	10.5	23.6	49.8	2.8	14.6	12.2	110.3	226.3	72 64	24	3	125	
POMDO	30–43 56, 60	B/A	n.d.	0.1	2.0	8.8	21.7	45.2	2.1	13.3	9.9	94.4	197.5	64 48	22 14	2	108	
POMD0 POMD0	56–69 70–80	Bw Cr	6.6 n.d.	0.1 0.1	1.4 1.4	7.9 9.7	14.0 10.4	31.4 15.4	1.0 0.5	9.3 7.8	8.2 9.4	91.2 83.6	164.4 138.3	48 35	14 10	1 1	100 91	
							10.1	10.1	0.0	, .0	2.1	55.0	100.0	55	-0	•	- 4	
	on rate 35.7 mm		-			-												
POMD4	0–5	A	5.9	0.29	20.7	6.2	54.2	87.5	6.5	23.5	28.4	153.3	380.7	122	54	6	177	
POMD4	5–10	A	5.6	0.11	2.5	13.5	38.5	74.7	5.0	22.0	23.0	148.8	328.1	111	38	5	171	
POMD4	10–17	Bw	n.d.	0.07	4.9	7.7	35.7	73.1	4.1	21.2	31.8	147.9	326.4	113	36	4	169	
POMD4	17–27	Bw	n.d.	0.11	3.1	9.1 5.5	29.2	77.5	4.6	21.6	25.1	143.8	314.1	112	29 27	5 4	165	
POMD4 POMD4	27–37	Bw	5.8	0.07	4.7	5.5	26.8 26.6	68.7	4.0	23.2	42.9 39.3	136.5 133.8	312.4 302.7	117 110	27 27	4 3	160 153	
POMD4 POMD4	37–51 51–75	Bw Cr	n.d. 5.9	0.11 0.14	9.6 0.6	0.0 7.1	24.2	71.1 68.0	3.4 2.7	18.8 18.6	39.3	133.8	290.0	108	27 24	3	153	
POMD4 POMD4	75–86	Cr	n.d.	0.14	4.6	2.2	27.6	39.7	1.5	20.6	30.0	135.6	274.2	72	28	3 1	168	
POMD4 POMD4	125–132	Cr	n.d.	0.14	4.0	3.2	29.2	23.1	3.5	23.9	24.1	110.7	221.9	50	29	4	135	
POMD4	140–148	Cr	n.d.	0.11	8.6	0.1	27.9	25.1	4.5	22.7	17.3	88.3	194.5	42	28	4	111	
POMD4	156–162	Cr	n.d.	0.07	6.5	1.9	32.0	30.4	5.7	26.4	21.5	101.3	225.8	54	32	6	128	
POMD4	165–177	Cr	n.d.	0.11	4.6	6.0	31.1	36.2	6.9	29.6	26.8	110.8	252.0	69	31	7	140	
. 0.1111	-00 1//			V.11	0	5.0	01.1	00.2	0.5	22.0	20.0	110.0	202.0	0,7	01	,	1.0	

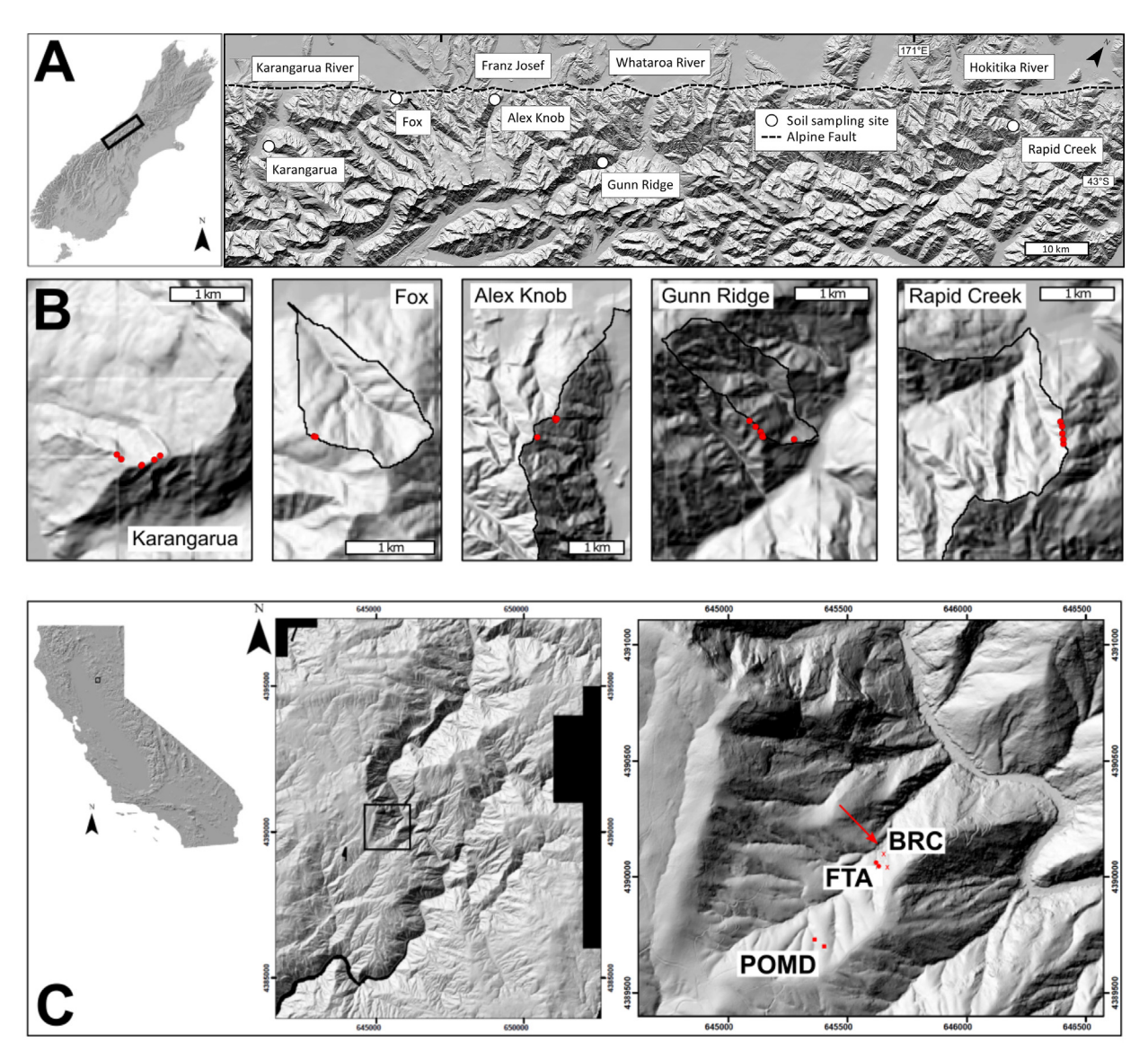


Fig. 2. Locations of the study areas in the western Southern Alps/New Zealand (WSA) and the Feather River/Northern Sierra Nevada, USA (FR). A) Overview of the sample locations of the WSA sites; B) detailed setting of each WSA soil pit on local ridge positions; C) overview and sample locations of the FR sites. The arrow in C) indicates the current position of the knick point.

The second study area is in the Feather River catchment (FR) in the Northern Sierra Nevada of California, USA (Fig. 2). The FR site is within the lower reaches of the Middle Fork Feather River, where mean annual precipitation is 1750 mm and the mean annual temperature 12.5 °C (PRISM Climate Group, www.prism.oregonstate.edu). The bedrock at the study site is granodiorite, but the adjacent area features a complex intrusion of granitoid plutons into metamorphic and ophilitic rocks (Saucedo and Wagner, 1992). Erosion rates vary with topography, with lower erosion rates of 20–40 mm ky $^{-1}$ for a relatively flat relict upland surface and high erosion rates of 200–250 mm ky $^{-1}$ on the steep slopes draining to the deeply incised canyon of the Feather River (Hurst et al., 2012; Riebe et al., 2000; Wakabayashi and Sawyer, 2001).

The FR study sites are located within the Bald Rock tributary basin that descends from a relict surface (850 m asl) to the Middle Fork Feather River (310 m asl). Spatially detailed rainfall data are lacking in the region. However, the region's precipitation map (Western Regional Climate Center, https://wrcc.dri.edu/Climate/maps.php) suggests that the elevation difference within the tributary basin causes only ~15% of variation in the annual mean precipitation. Relatively constant climate within the basin is also reflected in homogenous presence of mixed conifer forest (Milodowski et al., 2014). The overall slope gradients of

the FR sites within the tributary basin increase from approximately 15° to 31° toward the Middle Fork Feather River. A knick-point, which has been initiated by the incision of the Middle Fork Feather River, has been migrating upward through the tributary basin (Attal et al., 2015). Our sites comprise three eroding hillslope transects: POMD is near a low relief plateau and located above the knick-point, BRC is below the knick-point, and FTA is between the knick-point and the plateau. According to Hurst et al. (2012), catchment scale erosion rates adequately represent the spatial variability of erosion rates within the tributary basins and vary from 35.7 mm ky⁻¹ at POMD to 250 mm ky⁻¹ at BRC, with intermediate rates at the FTA sites. Since the soil thicknesses of the FTA soils do not differ significantly from those of POMD and BRC, they will have soil residence times that are between those of POMD and BRC (Table 2). Consistent with the range of residence times, all soils are Inceptisols. The BRC soils with highest erosion rates have substantially more coarse grain sizes and are more heterogeneous in their thicknesses as compared to POMD and FTA (Wang et al., 2018). Unlike POMD and FTA, which have continuous soil cover, BRC is also characterised by patchy bedrock outcrops (Milodowski et al., 2015). Though a generally negative relationship between soil thickness and erosion rate has been observed at an adjacent ridge line (Gabet et al., 2015), within the Bald

Rock Basin soil thickness is relatively insensitive to erosion rate (Yoo et al., 2011).

With respect to our conceptual framework of hillslope soils (Fig. 1), we define soil as the sum of pedogenic A and B horizons (Soil Survey Staff, 2014). Our field observations clearly indicated the effects of physical disturbance by tree roots and tree throws in mixing these horizons, qualifying the sum of A and B horizons as the mobile soil. The zone of chemical weathering between the soil and fresh bedrock, which is termed saprolite (Fig. 1), is characterised in our study areas by wellpreserved rock fabric indicative of minimal physical disturbance. At WSA, the thin $(< 0.5 \,\mathrm{m})$ saprolite zone can be at times better described as R horizon that comprises in-situ (i.e., physically connected to bedrock below), minimally weathered bedrock, and mm-sized cracks containing material from the overlying B horizon. At the WSA sites we took bulk-samples (combined A and B horizons) of each soil profile (one sample per site, total 22 samples from 22 soil sites). We took great care to obtain bulk samples that represented the true proportions of each soil horizon in the soils (i.e., no preferential sampling of one horizon) by cutting back the profile face with a spade over the entire depth of the soil and collecting the cut-back material. At the FR site each hillslope (POMD, FTA, BRC) was sampled at the summit, shoulder, and backslope for soil and saprolite material (convex to straight slopes). Each soil pit was excavated to the depth of 20-30 cm below the soil-saprolite boundary and soil samples were collected by horizons and depth intervals. Because little differences in soil geochemistry and morphology were observed as a function of topographic locations within each hillslope group (Yoo et al., 2011), our detailed P fractionation measurements were limited to two soil profiles from each hillslope.

2.3. Laboratory methods

We primarily present P data of soil samples and saprolite (FR only) for the following fractions: total P (Ptotal), the primary, apatite-derived P fraction (P_{apatite}), organic P as the organically bound P (P_{org}), the nonoccluded, iron and aluminium oxide-bound P (P_{Fe/Al}), and the occluded/recalcitrant/residual P fraction (Pocc). The extraction procedures differed between the WSA and FR sites due to the dates when the analyses were conducted (WSA in 2013, FR in 2016). For the WSA sites, P_{total} was extracted by NaOH fusion in nickel crucibles (Blakemore et al., 1987; Smith and Bain, 1982), and the extracts analysed following Murphy and Riley (1962). Porg was extracted following the ignition method of Saunders and Williams (1955). The modified Hedley sequential fractionation with 0.1 M NaOH and 1 M HCl after Tiessen and Moir (1993) yielded inorganic P_{Fe/Al} and P_{apatite}, respectively. P_{org}, P_{Fe/} Al, and Papatite extracts were quantified also following Murphy and Riley (1962). The difference between total P and the sum of P_{org} , $P_{apatite}$, and P_{Fe/Al} is regarded as the occluded/recalcitrant/residual P (P_{occ}). We note that our Pocc fraction does not discriminate between inorganic and organic P_{occ}.

The FR samples underwent a more detailed fractionation than the WSA samples following the scheme by Condron et al. (1996). This scheme involves a sequential extraction of 6 consecutive steps on the same soil sample: 1) extraction of labile inorganic P with 1 M ammonium chloride (Pi_{NH4Cl}); 2) inorganic and organic P (Pi_{bic} and Po_{bic}) with 0.5 M sodium bicarbonate (NaHCO $_3$ at pH 8.5); 3) inorganic and organic P (Pi_{OH} I and Po_{OH} I) with 0.1 M NaOH; 4) $P_{apatite}$ (Pi_{HCl}) with 1 M HCl; 5) a second extraction with 0.1 M NaOH (Pi_{OH} II and Po_{OH} II); and a final digestion with concentrated P_2 O4 and P_2 O5 to yield the residual P (Olsen and Sommers, 1982). The inorganic P concentration in acid extracts was quantified following Murphy and Riley (1962). Inorganic P in alkaline extracts followed Dick and Tabatabai (1977), whereas the organic P was obtained by the difference between the inorganic P and total P concentrations after digestion with ammonium persulfate and P_2 O4 in an autoclave.

To allow for comparability, the FR P fractions were combined to be equivalent to the WSA fractions: organic P (P_{org}) is the sum of Po_{bic} .

 $Po_{OH,I}$ and $Po_{OH,II}$; apatite P ($P_{apatite}$) is equivalent to Pi_{HCI} ; $P_{Fe/Al}$ is $Pi_{OH,II}$; and occluded P (P_{occ}) equals the sum of $Pi_{OH,II}$ and $P_{residual}$ (here we account for the fact that the simpler P fractionation of the WSA samples does not include a second NaOH extraction that was performed on the Feather River samples). P data are only reported for the mineral horizons (Table 1 for WSA and Table 2 for FR). At both sites we measured pH of the bulk samples (WSA) and selected depth increments (FR) at a soil/water mass ratio of 1:2.5. To compare results between the two sites and previous work, we focus on the ratios of $P_{apatite}$, P_{occ} , P_{org} , and $P_{Fe/Al}$ to P_{total} rather than absolute P concentrations, as this approach allows comparison of sites with varying concentrations of P in the parent material (Hahm et al., 2014; Mage and Porder, 2013; Porder and Ramachandran, 2013). Regression analysis and derivation of regression model parameters was conducted using R (R Core Team, 2017).

3. Results

3.1. Western Southern Alps, New Zealand

Soils are very acidic (Table 1) with pH values as low as 3.2, similar to other published data from the region (e.g., Almond and Tonkin, 1999; Stevens, 1968; Tonkin and Basher, 2001). Since these are composite values representing the substrate over the entire depth of each soil, the values are likely to be lower for the topsoils and higher for the subsoils alone. Secondary P is the predominant form of P in the WSA samples (83–97%), whereas apatite P remains between 3% to 17% of Ptotal over the entire range of soil residence times (Fig. 3, Table 1). The Papatite/Ptotal ratio is weakly inversely correlated with soil residence time (χ) (Papatite/Ptotal = 0.1144 $^{-0.0002\chi}$, R² = 0.18, p = 0.045). In contrast, neither Porg nor P mainly associated with pedogenic oxides (Pocc and PFe/AI) are statistically significantly correlated with residence time.

3.2. Feather River, California, USA

Soils at FR are slightly acidic throughout. At the FR sites (Fig. 3), depth-weighted contributions of P fractions to P_{total} of each soil show $P_{apatite}$ is always < 3% of $P_{total}\text{,}$ whereas P_{org} and P_{occ} are clearly dominant. The high proportions of $P_{\rm org}$ and $P_{\rm occ}$ are present across the range of soil residence times (Fig. 3). Only Porg decreases slightly with increasing soil residence time (χ) following a statistically significant power-law model ($P_{org}/P_{total}=0.76\chi^{-0.113}$ $R^2=0.89,~p<0.005$). Since P fractions are measured in consecutive depth intervals and soils are deeper at the FR sites than the WSA sites, a more detailed picture of the P fractions across soil depths was obtained (Fig. 4). Despite the rudimentary morphological development of the Inceptisols, there are major depth gradients in P chemistry. Nearly all P fractions and Ptotal have highest concentrations in the topsoil (Fig. 4, Table 2). High topsoil concentrations are most strongly expressed in the more bio-available secondary forms of P (NH₄Cl, NaHCO₃, and first NaOH extractions) but also Papatite. The decline for most P fractions with depth continues beyond the soil and reaches deep (> 200 cm) into the saprolite (Cr) with the exception of Papatite concentrations, which increase again in concentration at depths > 150 cm.

4. Discussion

4.1. Soil P relative to soil residence time vs. soil age

Soil residence times vary by up to four orders of magnitude but residence times exert little control on the concentrations of total P; $P_{apatite}/P_{total}$ ratios remain low (< 18% at WSA, < 3% at FR) for all soils (Tables 1 and 2). The statistically significant model linking soil residence time to $P_{apatite}/P_{total}$, albeit statistically weak, indicates that the paradigm of $P_{apatite}$ loss with increasing soil development time cannot be rejected at least for WSA. However, at WSA the proportion of

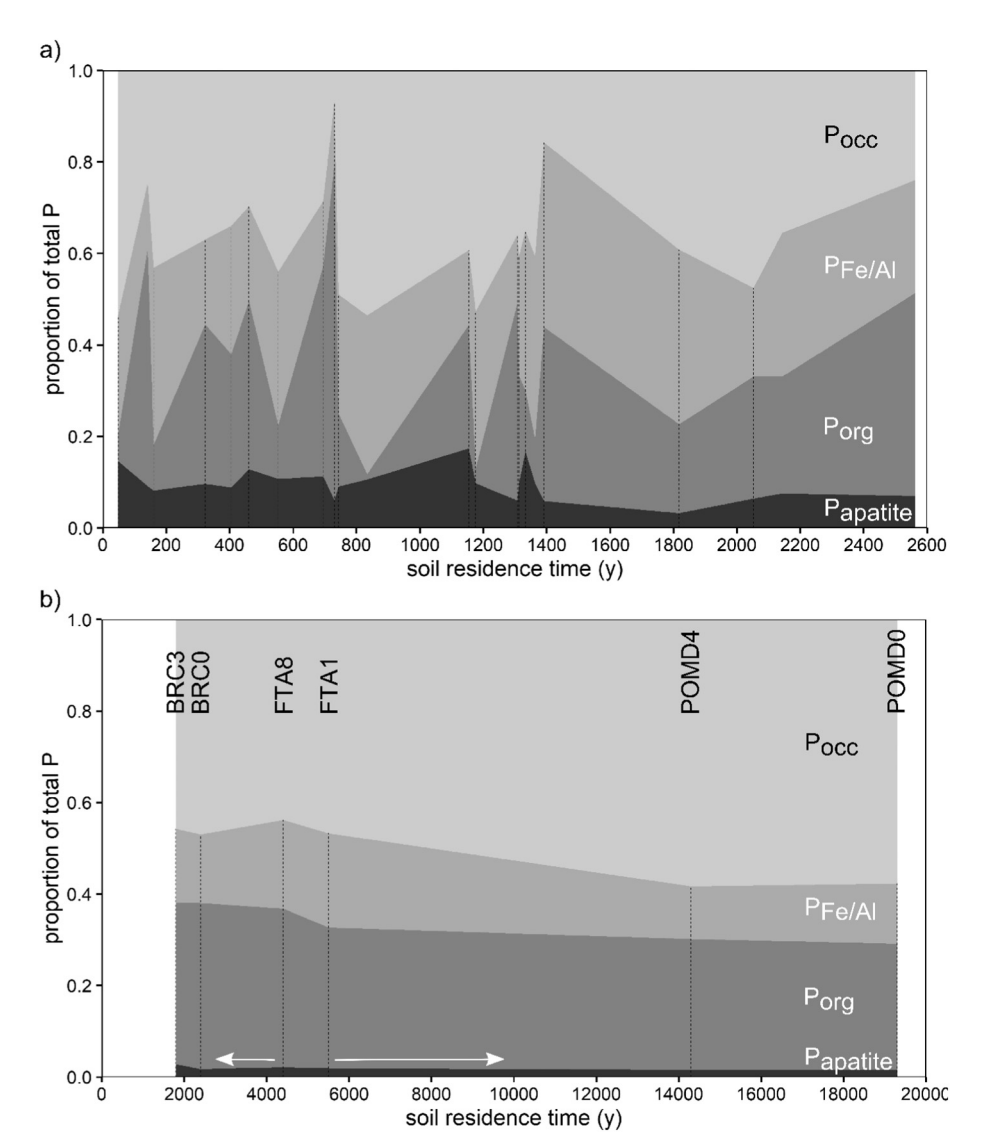


Fig. 3. Relative contributions of soil P fractions to P_{total} in a) WSA soils and b) FR soils as a function of soil residence times. Dotted lines indicate the individual sites across the gradients. The white arrows in b) indicate the potential range of soil residence time of the FTA sites as intermediate between the BRC and POMD values. The FTA soil residence times are used for illustration purposes are derived from the average of the erosion rates of 35.7 mm ky⁻¹ (POMD) and 250 mm ky⁻¹ (BRC). Soil residence time has little influence on P fractions and secondary P fractions clearly dominate over $P_{apatite}$ at all times.

 $P_{apatite} \ to \ P_{total} \ at \ the \ shortest \ soil \ residence \ time \ is < 18\% \ in \ contrast \ to \ the \ classic \ Walker \ \& \ Syers \ paradigm \ that \ predicts \ the \ dominance \ of \ P_{apatite} \ over \ secondary \ P \ forms \ in \ such \ young \ soils \ with \ rudimentary \ profile \ morphology \ (Entisols, Inceptisols).$

In Fig. 5, we compared our own ratios of $P_{apatite}/P_{total}$ as a function of soil residence time to the published ratios from soil chronosequence studies. It appears that soils at both of our study sites, despite not being morphologically developed beyond Inceptisols, have already reached the late stage of soil P development with a very low and largely invariant proportion of $P_{apatite}$ and very high secondary P forms typical for older chronosequence sites (Fig. 5). For instance, contrasting the WSA sites against the Spodosols developed on the nearby Franz Josef chronosequence shows that the 10% average proportion of $P_{apatite}$ in the WSA soils is at best similar to the top 30 cm (to stay within our range of WSA soil depths) of > 1000- to 5000-year-old soils of the Franz Josef chronosequence (Stevens, 1968). Additionally, the P_{occ}/P_{total} ratios of the hillslope soils at WSA are so high that they are only replicated at the 120,000 y-old, retrogressive stage of the Franz Josef chronosequence (data from Stevens, 1968).

Contrasting the FR sites to the Merced River chronosequence (Harden, 1987), developed on granite-derived alluvium and located just

west of the Sierra Nevada, reveals that, like the WSA, the P chemistry of hillslope soils is comparable to that of old soils. We note here that the Merced River sites developed in a dryer climate than the FR sites (mean annual precipitation: 300 mm). Although P fractionation data are not available for the Merced River chronosequence, the site's apatite concentrations can serve as a proxy for the depletion of primary mineral P (Papatite) (Harden, 1987). Apatite concentrations in Merced River soils decrease 10-fold within the first 40 ky of soil formation with little change thereafter (> 40 ky to 600 ky). The initially rapid decline of apatite observed at the Merced River chronosequence is similar to the trend in Papatite depletion at Franz Josef and other chronosequences (Fig. 5). Comparing the FR sites to Merced River chronosequence, the low and invariant contributions of Papatite to Ptotal at the FR site signals that FR soils have already reached that stage of severe apatite depletion only observed in Merced River soils older than 40 ky that exhibit much greater morphological maturity and chemical differentiation (e.g. layers of illuvial clay-enrichment in the soil) than the FR hillslope soils.

The only other published P fractionation data in Fig. 5 from eroding hillslopes with temporal data are from Puerto Rico (McClintock et al., 2015). McClintock et al. (2015) reported soil residence time for the top 20 cm of soils and every sample contained < 5% of $P_{apatite}$ (their HCl-

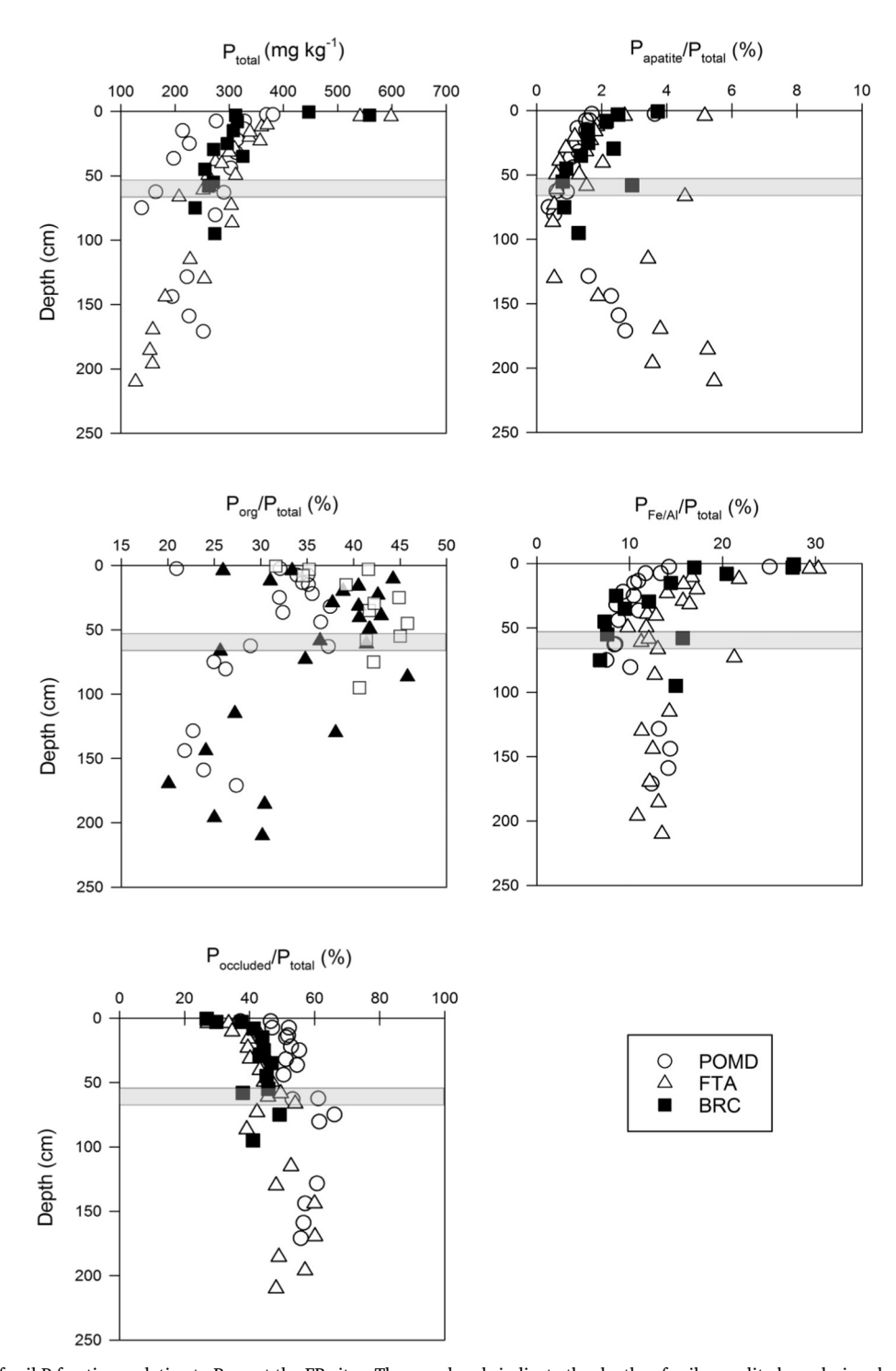


Fig. 4. Depth profiles of soil P fractions relative to P_{total} at the FR sites. The grey bands indicate the depths of soil-saprolite boundaries observed at the FR sites. The general decline of concentrations with depth toward the saprolite appears to be a uniform feature independent of the soil residence time. Only P_{apatite} increases again below 150 cm. See Table 2 for individual values.

extractable P). $P_{\rm occ}$ (residual-P), $P_{\rm org}$ (NaHCO₃-P_o + NaOH-P_o) and $P_{\rm Fe/Al}$ (NaOH-P_i) contribute on average 55%, 30%, and 13% to $P_{\rm total}$, respectively. The residence times of their soils are comparable to those we studied (Fig. 5), and there is also similarity to our average P inventory that shows the contributions to $P_{\rm total}$ of $P_{\rm occ} > P_{\rm org} = P_{\rm Fe/Al}$ for WSA and $P_{\rm occ} > P_{\rm org} > P_{\rm Fe/Al}$ for FR (Fig. 3). These similar patterns in soil P persist despite the large climatic difference between WSA, FR and Puerto Rico (Fig. 6), indicating that climate is not a driver of such patterns observed in P fractions.

4.2. Comparison to published soil P data from eroding hillslopes

Our results differ from the patterns reported for soil chronosequence studies (Fig. 5) but are consistent with soil P fractionation studies conducted on eroding hillslopes underlain by crystalline bedrock (Fig. 7). These published data are compiled from studies that explicitly describe soil sampling locations on hillslopes and from in-situ soil parent materials (or local regolith). Most sites in Fig. 7 are upslope locations where soil production from the underlying bedrock maintains

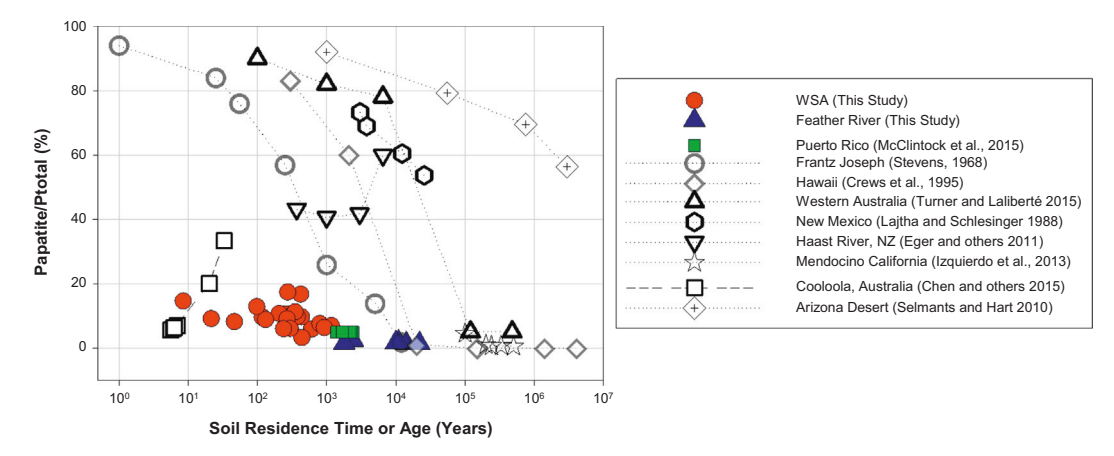


Fig. 5. Relative contributions of P_{apatite} to P_{total} across soil residence time and soil age gradients (filled solid points denote studies on hillslope soils, whereas hollow points are chronosequence studies).

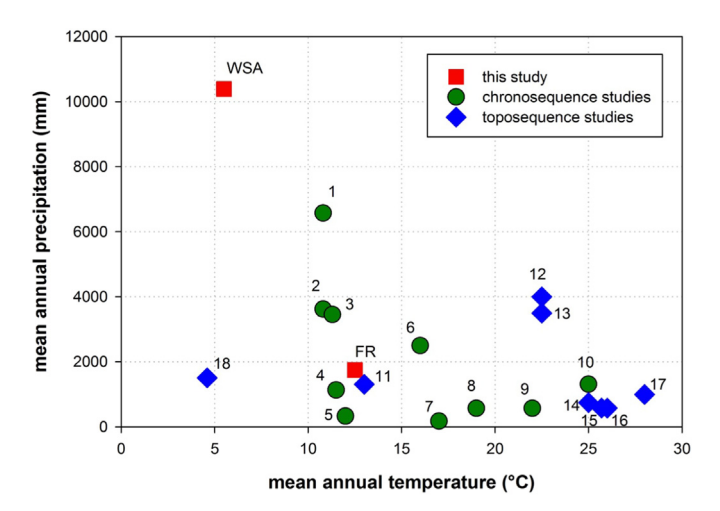


Fig. 6. Climate data from the sites discussed in this study (Figs. 8 and 9). References as follows: 1, 2 Franz Josef, NZ (Richardson et al., 2004) 3 Haast River, NZ (Eger et al., 2011); 4 Mendocino, California (Izquierdo et al., 2013); 5 Arizona desert (Selmants and Hart, 2010); 6 Hawaii (Crews et al., 1995); 7 New Mexico (Lajtha and Schlesinger, 1988); 8, 9 Western Australia (Turner and Laliberté, 2015); 10 Northern Brazil (Agbenin and Tiessen, 1994); 11 Hawaii (Vitousek et al., 2003); 12 Puerto Rico (McClintock et al., 2015); 13 Puerto Rico (Mage and Porder, 2013); 14 Cooloola, AUS (Chen et al., 2015); 15, 16 Northern Brazil (Araújo et al., 2004); 17 Ghana (Abekoe and Tiessen, 1998); 18 Sierra Nevada, California (Homyak et al., 2014).

soil cover and colluvial deposition is limited. All soils from eroding hillslopes in the published literature, despite their presumably short soil residence times due to erosion, have very low percentages of $P_{apatite}$ (Fig. 7). Eroding soils also contain a high proportion of P_{occ} relative to P_{total} (Abekoe and Tiessen, 1998; Araújo et al., 2004; Homyak et al., 2014; Mage and Porder, 2013; McClintock et al., 2015; Vitousek et al., 2003), consistent with results from the WSA and FR sites.

In Fig. 7, the soils from semi-arid northern Brazil (Agbenin and Tiessen, 1994) are an exception to the low contribution of $P_{\rm apatite}$ to $P_{\rm total}$ in eroding soils. The $P_{\rm apatite}$ contribution to $P_{\rm total}$ in A horizons of these upslope soils reaches 60 \pm 18% in shallow Entisols, but that quickly decreases to 17 \pm 18% lower on the slope where thick depositional Inceptisols are found. However, this northern Brazilian hill-slope (Agbenin and Tiessen, 1994) is underlain by apatite-rich syenite that is unusual for the region (Araújo et al., 2004). In summary, excluding the study site underlain by apatite-rich syenite, no previous work from eroding hillslopes we examined documents $P_{\rm apatite}$ contributing > 30% of $P_{\rm total}$.

Despite the extreme rainfall rates, it seems unlikely that the strong

depletion of $P_{apatite}$ at WSA is simply a reflection of the high rainfall in accelerating the weathering and transformation of rock/soil P. Fig. 7 shows the range of precipitation from the published hillslope P studies including those from this study. It is clear that the exceedingly low contribution of apatite to total P on eroding hillslopes is not limited to regions of high rainfall but rather is a norm across a wide range of precipitation rates.

Although they did not measure phosphorus, Dixon et al. (2009) linked erosion rates and chemical weathering state of soils and saprolite. They found that the chemical weathering state of the saprolite determined the chemical weathering of the soil: when the saprolite was highly weathered, additional weathering in the soil was low, whereas when the saprolite was only weakly chemically altered, the contribution of soil weathering to the overall chemical weathering of the weathering column would be high. Given that Dixon et al. (2009) found a strong relationship between erosion rate and weathering rate of the saprolite (but not the soil), we expected that the P inventory of the saprolite at FR would respond to erosion rates. However, this (i.e., higher erosion rates/lower residence times = less strongly depleted apatite P in the saprolite) does not seem to be the case at FR (see saprolite samples in Table 2).

4.3. Potential effects of aeolian P input

One potential contribution to the P depth profiles we see (e.g., the increase in total P from saprolite to soil observed at FR; Fig. 4) is dust deposition. Substantial dust deposition is highly unlikely for the WSA sites, as studies have shown that even in favourable conditions of local dust mobilisation (e.g. close to an unvegetated braided river in the coastal plain) any effect of dust on soil P is limited to areas close to the dust source (< 2 km) (Eger et al., 2013a). There is no local dust-producing source in the vicinity of our WSA sites and long-range deposition from Australia (Holocene dust deposition rate 0.6 g m⁻² y⁻¹; Marx et al., 2009) will have little impact at such high erosion rates (lowest rate of all WSA soils 307 g m⁻² y⁻¹; Larsen et al., 2014a). For the FR sites, as indicated by the peaks of most P fractions and Ptotal in the topsoil, deposition of dust may be more significant even in eroding (and thus rejuvenating) soils. Aciego et al. (2017) extrapolated a threemonth dust trapping record from the driest months in the Sierra Nevada to annual deposition rates of 3 to 36 g m⁻². Hence, although this extrapolation might be an overestimation due to limiting the measurements to the dry season, we acknowledge the likely accretion of Pbearing dust in the FR study area. However, dust deposition has little effect on our interpretation. With increasing soil depth, closer to the parent material source, and decreasing potential impact of atmospheric deposition, the P_{apatite} remains low and secondary P forms remain clearly dominant regardless of soil residence time (Fig. 4). Alternative

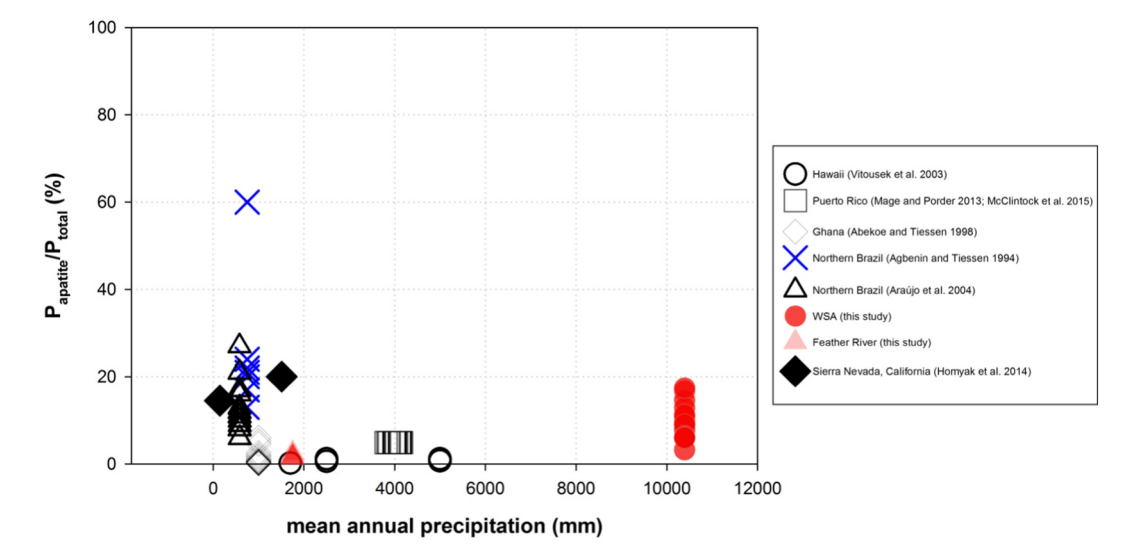


Fig. 7. Contribution of $P_{apatite}$ to P_{total} versus mean annual precipitation for eroding hillslope soils from this study and from the literature. In plotting published data, we did not attempt to average the reported values or combine results from different depths for calculating soil profile integrated values. Instead all of the reported values are included in this figure. For the study conducted in the high Sierra Nevada (Homyak et al., 2014), we note that their reported P values are averaged over several soil profiles that include soils on hillslopes and adjacent depositional settings.

or complementary explanations for the surface peak in P concentrations include P uplift by plants (Jobbágy and Jackson, 2004) or bioturbation within the soil (e.g., frequently observed tree throw in the study area).

4.4. Soil P and soil order

All of the soils at our field sites are either Entisols or Inceptisols. Nevertheless, they are highly depleted in Papatite. Our data are largely consistent with other soil P studies conducted for eroding hillslopes (Fig. 8a). These observations clearly deviate from the general relationship of P fractions and soil orders postulated first by Smeck (1985), which is a pedological extension of the Walker and Syers (1976) paradigm, such that the progressive change of soil orders is aligned with the predictable changes in soil P. Soils are assumed to develop in a sequence from Entisols to Inceptisols to Alfisols to Ultisols (or Spodosols) to Oxisols (Smeck, 1985). The concept of correlation between soil P fractions and soil orders was later confirmed through global data compilations (Cross and Schlesinger, 1995; Lajtha and Schlesinger, 1988; Yang and Post, 2011). However, most of the data sets used to build these relationships between P fractions and soil order are from geomorphically stable landforms. In contrast, data from eroding hillslopes, regardless of soil order, show low P_{apatite} contributions to P_{total} (Fig. 8a). Consequently, neither soil residence time nor soil order is able to predict the low Papatite contributions on eroding, soil-mantled hillslopes.

4.5. Why do soil order and soil residence time fail to explain the contribution of $P_{apatite}$?

Whereas soil residence time on eroding hillslopes explains the dominance of soil orders typical of young geomorphic surfaces, it fails to account for the low contribution of $P_{apatite}$ to P_{total} .

Soil order is determined largely by field observations of soil morphology including soil colour coatings, texture, structure, and horizons. The vertical depth distribution of these morphological properties is particularly diagnostic for several soil orders. For example, vertical distribution of soil texture and B horizon development are critical for determining a series of soils from Inceptisols to Ultisols (Soil Survey Staff, 2014). Continual mixing and/or consequent rejuvenation of a soil by erosion and soil production, for instance, would physically prevent the development of such vertical properties, similar to the effects of bioturbation (Johnson and Watson-Stegner, 1987). Because of this, soil

orders characteristic for young geomorphic surfaces can develop from strongly weathered parent material as long as soil residence time is short and thus prevent significant vertical horizonation within the soils. It is also notable that the only soil order that is associated with mature soil development in Fig. 8a is the Oxisol. This is because in soil taxonomy, Oxisols, unlike Ultisols, do not require strong vertical stratification in clay contents and the classification is largely dependent on heavily-weathered soil minerals. The observation that soil order can be decoupled from weathering state of the parent material is not limited to eroding hillslopes. At the Cooloola sand dune soil chronosequence in Australia (Chen et al., 2015) (Fig. 8b), unlike at most other soil chronosequences, the young Entisols exhibits low levels of apatite P, simply because highly weathered sand deposits constitute the site's soil parent material.

The insensitivity of soil order to pre-weathering in parent material is consistent with our sites where Entisols and Inceptisols have formed from already chemically weathered saprolite. This is evident from the FR data (Fig. 4), where the soils have not formed from fresh bedrock but from saprolite overlying unweathered granodiorite. The saprolite weathering is evident by the dominance of secondary P forms (Fig. 4) and enrichment in biogeochemically conservative elements such as Zr (Yoo et al., 2011). We did not reach the depth to fresh bedrock despite hand augering to depths of 2 to 9 m below the soil-saprolite boundary.

Therefore at least for eroding, soil mantled hillslopes, available data suggest that soil P dynamics neither proceed in tandem with the general developmental sequence of soil orders as proposed by Smeck (1985) nor make soil residence time a good predictor of soil P dynamics.

We believe the reason for the discrepancy between chronosequences and hillslopes is derived from a fundamental difference between 'erosional' soils and 'depositional' soils. In contrast to hillslope soils, most chronosequences are originally developed in relatively unweathered parent material of water-, and glacier-transported origin. These transport mechanisms usually comprise comminution and particle size sorting. Deposition of lighter and more weathered mineral particles (clays, oxides) in the lowlands becomes less likely since these particles offer less resistance to physical transport (Dellinger et al., 2014; Kautz and Martin, 2007). Instead, the less weathered particles of mostly larger size fractions (silt, sand, > 2 mm) preferentially accumulate and ultimately form the parent material of lowland chronosequences (e.g., see parent material of chronosequence soils from NZ and California: Eger et al., 2011; Harden, 1987; Ross et al., 1977; Stevens, 1968; Wells and Goff, 2007).

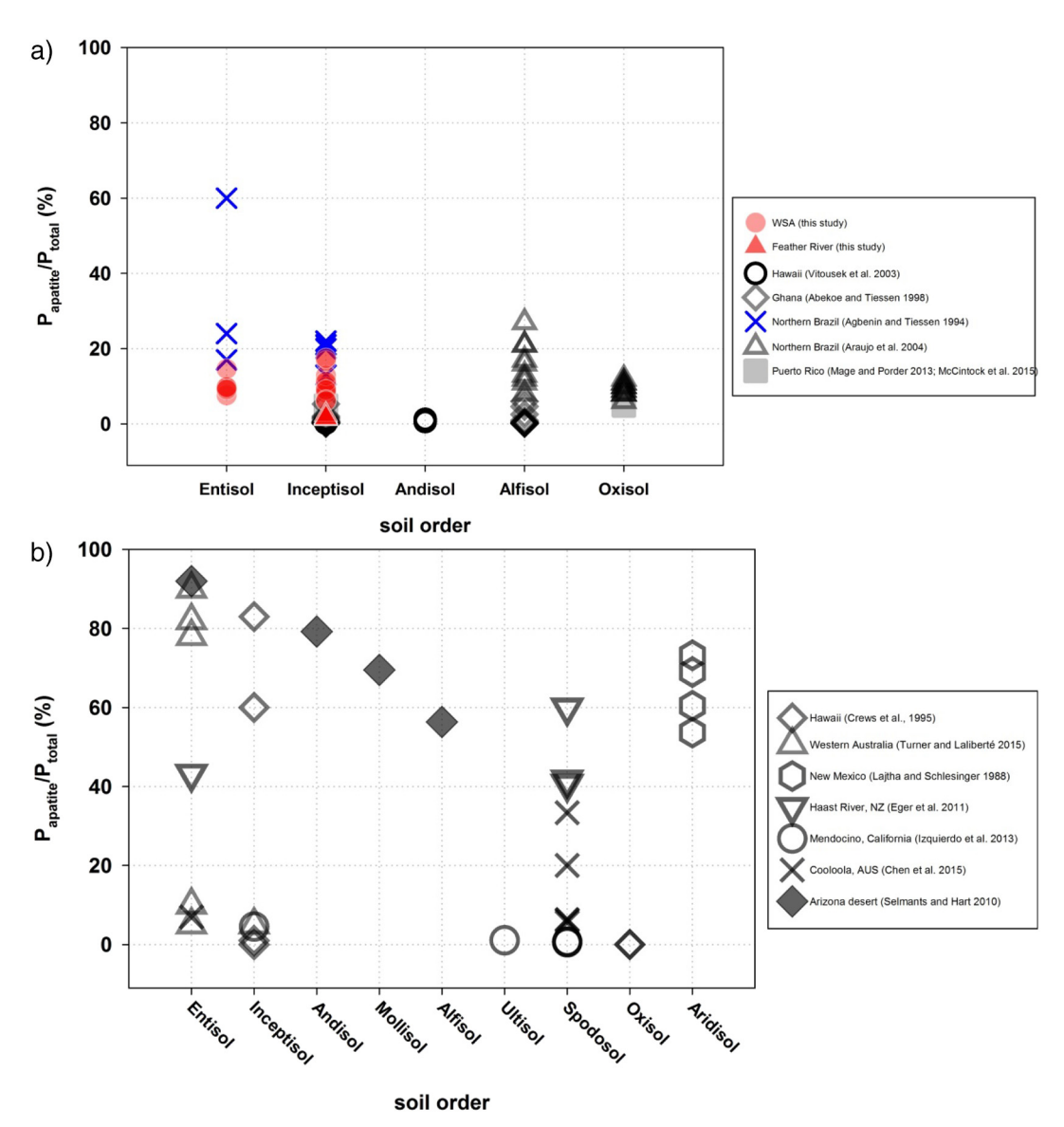


Fig. 8. Soil $P_{apatite}/P_{total}$ plotted against soil orders for a) eroding hillslopes, and b) soil chronosequences.

Chronosequences that are formed from volcanic rocks, like in Hawaii (Crews et al., 1995; Vitousek, 2004), behave similar to chronosequences developed from sedimentary lithologies: lava flows in Hawaii create new, minimally eroding geomorphic surfaces from initially unweathered, Papatite-rich parent material, conceptually similar to chronosequences on sedimentary deposits that involve particle sizedifferentiating transport (Fig. 5). To our knowledge, the Cooloola coastal dune sequence is the only published soil chronosequence with P fractionation data derived from a pre-weathered allochthonous parent material. Not unlike our residence time gradients, it shows low and invariant P_{anatite} values across the entire sequence (Chen et al., 2015). Thus, both concepts, soil residence time and soil age in their narrow definitions do not consider any pre-weathering of parent material. However, soil age is often able to structure the evolution of soils on chronosequences because the parent material at the start of soil formation is usually minimally weathered.

4.6. Vertical distribution of P fractions

It has been proposed (Porder et al., 2007a; Uhlig and von Blanckenburg, 2016) that a 'vertically oriented' version of the Walker and Syers (1976) model of P evolution applies to the changes of P

fractions with depth (Fig. 9A). Such model recognises the inverse relationship between soil depth and mineral age following the incorporation of minerals into the active weathering zone of saprolite and soil.

However, the FR data and the review of existing studies allow this model to be modified at multiple fronts. In contrast to the expectation from the vertically oriented Walker and Syers model, total P does not gradually increase with increasing soil depth (Fig. 9B). Our data from FR (Fig. 4) indicate that total P decreases as bedrock chemically weathers to saprolite but that total P is greater in soils than in saprolite, albeit soil P dominated by secondary P forms. We attribute higher soil P concentrations to two processes: 1) dust deposition, and 2) biological nutrient redistribution (nutrient uplift) (Jobbágy and Jackson, 2004), whereby roots propagate into the saprolite and take up bio-available P from the saprolite zone. Plant-bound P is then returned to the soil as organic P, and partly transformed into other secondary (inorganic) P forms. Enrichment of P in surface soils associated with biological nutrient uptake and/or atmospheric deposition has been commonly observed (Chadwick and Asner, 2016; Merritts et al., 1992; Yoo et al., 2015) and does not seem to be necessarily limited to a particular P fraction or geomorphic setting (slopes vs. chronosequences) (Agbenin and Tiessen, 1994; Homyak et al., 2014; Lajtha and Schlesinger, 1988;

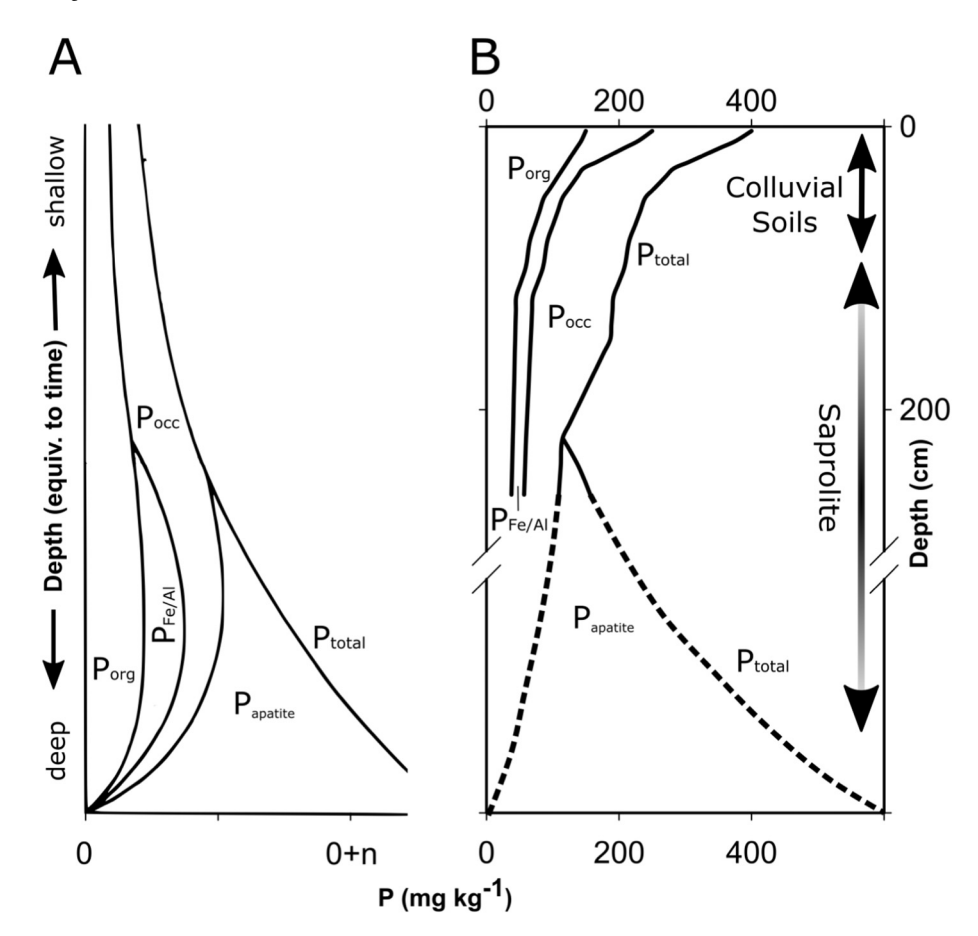


Fig. 9. A) Vertically oriented Walker and Syers model and B) a new P dynamics model for weathering profiles based on the results from the Feather River sites. The WSA data show a similar pattern but lack the same detailed depth resolution due to the different sampling protocols. Although, we did not measure P_{total} for fresh bedrock at the Feather River, globally compiled P contents of granodiorite bedrock types show mean value of 810 mg kg⁻¹ with 25% value of 480 and 75% value of 1004 mg kg⁻¹ (Porder and Ramachandran, 2013).

Mage and Porder, 2013; Stevens, 1968; Turner and Laliberté, 2015). Additionally, organic matter is concentrated in the top of the weathering profile which together with Fe/Al oxides and secondary silicate clays partly protects P from leaching through the formation of $P_{\rm org}$, $P_{\rm occ}$ and $P_{\rm Fe/Al}$. With increasing depth, the P-depleted saprolite zone beneath the enriched soil will eventually transition into more unweathered parent material with higher P concentrations and an increase of $P_{\rm apatite}$.

Therefore, it is not erosion directly that rejuvenates P. It is instead plant uptake of P at depth and dust deposition that rejuvenates soil P. Indirectly, erosion is required to maintain an ongoing supply of P to the root exploration zone of plants.

5. Conclusion

We characterised P fractionation in soils from eroding hillslopes across two soil residence time gradients and compared these new results against published soil P data from hillslopes and soil chronosequences on non-eroding landforms. We tested the Walker and Syers paradigm of soil P development as derived from soil chronosequences against hillslope soils through the conceptual link between soil residence times and soil ages. A naive application of this P model to eroding hillslopes predicts dominance of $P_{\rm apatite}$ over secondary P in soils with very short residence times. However, we find the majority of soil P we and others have measured exists in the form of secondary P (83-97% in our data) regardless of soil residence time. Furthermore, soil residence time also does not explain the distribution of the secondary P forms. We conclude that the fundamental difference between chronosequence and hillslope soil derives from the weathering occurring in the bedrock (formation of saprolite) before it becomes part of the mobile soil. During initial stages of chronosequence development P_{apatite} almost always dominates and P-depleted saprolite is normally not present. In contrast, on hillslopes weathered bedrock or saprolite

appears to be common, combined with soils of short residence times and immature soil development. The legacy of pre-soil weathering of the underlying saprolite effectively counteracts the fertilising potential of the tectonic uplift – soil erosion – soil production feedback. Our data also indicate that plants may play an important role in redistributing P by uplift from the saprolite zone to the soil. Together with external dust, this redistribution increases soil P concentrations relative to the saprolite. Our work suggests that limits on ecosystem development through a decline of bio-available soil P forms may be more relevant to eroding hillslope soils than previously thought.

Acknowledgements

We thank the Department of Conservation for granting permission to sample soils in New Zealand. AE, KY and PCA had the conceptual idea for the research, GB performed the majority of the P laboratory analysis, XW prepared the samples and data from Feather River, AE and KY lead the data interpretation and write-up with contributions of all co-authors. KY and SM designed and conducted sampling at Feather River. IL and AE collected the New Zealand samples with support from NSF (OISE-1015454 to IL). AE was partially supported through a Landcare Research Capability Fund grant. KY thanks NSF (EAR-1253198) for supporting his portion of this work. KY and SM appreciate help in the field from Beth Weinman, Martin Hurst, Manny Gabet, and Tony Dosseto. IL and AE are grateful to Brendon Malcolm for help in the field.

References

Abekoe, M.K., Tiessen, H., 1998. Fertilizer P transformations and P availability in hill-slope soils of northern Ghana. Nutr. Cycl. Agroecosyst. 52 (1), 45–54.

Aciego, S.M., Riebe, C.S., Hart, S.C., Blakowski, M.A., Carey, C.J., Aarons, S.M., Dove, N.C., Botthoff, J.K., Sims, K.W.W., Aronson, E.L., 2017. Dust outpaces bedrock in

- nutrient supply to montane forest ecosystems. Nat. Commun. 8.
- Agbenin, J.O., Tiessen, H., 1994. Phosphorus transformations in a toposequence of lithosols and cambisols from semi-arid northeastern Brazil. Geoderma 62 (4), 345–362.
- Almond, P.C., Tonkin, P.J., 1999. Pedogenesis by upbuilding in an extreme leaching and weathering environment, and slow loess accretion, South Westland, New Zealand. Geoderma 92 (1–2), 1–36.
- Almond, P., Roering, J., Hales, T.C., 2007. Using soil residence time to delineate spatial and temporal patterns of transient landscape response. J. Geophys. Res. Earth 112 (F3).
- Amundson, R., Heimsath, A., Owen, J., Yoo, K., Dietrich, W.E., 2015. Hillslope soils and vegetation. Geomorphology 234 (0), 122–132.
- Araújo, M.S.B., Schaefer, C.E.R., Sampaio, E.V.S.B., 2004. Soil phosphorus fractions from toposequences of semi-arid latosols and luvisols in northeastern Brazil. Geoderma 119 (3-4), 309–321.
- Arvin, L.J., Riebe, C.S., Aciego, S.M., Blakowski, M.A., 2017. Global patterns of dust and bedrock nutrient supply to montane ecosystems. Sci. Adv. 3 (12).
- Attal, M., Mudd, S.M., Hurst, M.D., Weinman, B., Yoo, K., Naylor, M., 2015. Impact of change in erosion rate and landscape steepness on hillslope and fluvial sediments grain size in the Feather River basin (Sierra Nevada, California). Earth Surf. Dyn. 3 (1), 201–222.
- Blake, L., Johnston, A.E., Poulton, P.R., Goulding, K.W.T., 2003. Changes in soil phosphorus fractions following positive and negative phosphorus balances for long periods. Plant Soil 254 (2), 245–261.
- Blakemore, L.C., Searle, B.K., Daly, B.K.N., 1987. Methods for chemical analysis of soils. In: Soil Bureau Scientific Report. 80.
- Boyle, J.F., Chiverrell, R.C., Norton, S.A., Plater, A.J., 2013. A leaky model of long-term soil phosphorus dynamics. Glob. Biogeochem. Cycles 27 (2), 516–525.
- Chadwick, K.D., Asner, G.P., 2016. Tropical soil nutrient distributions determined by biotic and hillslope processes. Biogeochemistry 127 (2–3), 273–289.
- Chadwick, O.A., Derry, L.A., Vitousek, P.M., Huebert, B.J., Hedin, L.O., 1999. Changing sources of nutrients during four million years of ecosystem development. Nature 397 (6719), 491–497.
- Chen, C.R., Hou, E.Q., Condron, L.M., Bacon, G., Esfandbod, M., Olley, J., Turner, B.L., 2015. Soil phosphorus fractionation and nutrient dynamics along the Cooloola coastal dune chronosequence, southern Queensland, Australia. Geoderma 257–258, 4–13.
- Condron, L.M., Cornforth, I.S., Davis, M.R., Newman, R.H., 1996. Influence of conifers on the forms of phosphorus in selected New Zealand grassland soils. Biol. Fertil. Soils 21 (1), 37–42.
- Crews, T.E., Kitayama, K., Fownes, J.H., Riley, R.H., Herbert, D.A., Mueller-Dombois, D., Vitousek, P.M., 1995. Changes in soil phosphorus fractions and ecosystem dynamics across a long chronosequence in Hawaii. Ecology 76 (5), 1407–1424.
- Cross, A.F., Schlesinger, W.H., 1995. A literature review and evaluation of the Hedley fractionation: applications to the biogeochemical cycle of soil phosphorus in natural ecosystems. Geoderma 64 (3–4), 197–214.
- Dellinger, M., Gaillardet, J., Bouchez, J., Calmels, D., Galy, V., Hilton, R.G., Louvat, P., France-Lanord, C., 2014. Lithium isotopes in large rivers reveal the cannibalistic nature of modern continental weathering and erosion. Earth Planet. Sci. Lett. 401, 359–372.
- Dere, A.L., White, T.S., April, R.H., Reynolds, B., Miller, T.E., Knapp, E.P., McKay, L.D., Brantley, S.L., 2013. Climate dependence of feldspar weathering in shale soils along a latitudinal gradient. Geochim. Cosmochim. Acta 122, 101–126.
- Dick, W.A., Tabatabai, M.A., 1977. Determination of orthophosphate in aqueous solutions containing labile organic and inorganic phosphorus compounds. J. Environ. Qual. 6 (1).
- Dixon, J.L., Heimsath, A.M., Amundson, R., 2009. The critical role of climate and saprolite weathering in landscape evolution. Earth Surf. Process. Landf. 34 (11), 1507–1521.
- Eger, A., Almond, P.C., Condron, L.M., 2011. Pedogenesis, soil mass balance, phosphorus dynamics and vegetation communities across a Holocene soil chronosequence in a super-humid climate, South Westland, New Zealand. Geoderma 163 (3–4), 185–196.
- Eger, A., Almond, P.C., Condron, L.M., 2013a. Phosphorus fertilization by active dust deposition in a super-humid, temperate environment—soil phosphorus fractionation and accession processes. Glob. Biogeochem. Cycles 27 (1), 108–118.
- Eger, A., Almond, P.C., Wells, A., Condron, L.M., 2013b. Quantifying ecosystem rejuvenation: foliar nutrient concentrations and vegetation communities across a dust gradient and a chronosequence. Plant Soil 367 (1), 93–109.
- Filippelli, G.M., 2002. The global phosphorus cycle. Rev. Mineral. Geochem. 48 (1), 391–425.
- Frossard, E., Condron, L.M., Oberson, A., Sinaj, S., Fardeau, J.C., 2000. Processes governing phosphorus availability in temperate soils. J. Environ. Qual. 29 (1).
- Gabet, E.J., Mudd, S.M., Milodowski, D.T., Yoo, K., Hurst, M.D., Dosseto, A., 2015. Local topography and erosion rate control regolith thickness along a ridgeline in the Sierra Nevada, California. Earth Surf. Process. Landf. 40 (13), 1779–1790.
- Gilbert, G.K., 1877. Report on the Geology of the Henry Mountains, Washington, D.C.Report on the Geology of the Henry Mountains, Washington, D.C.
- Green, E.G., Dietrich, W.E., Banfield, J.F., 2006. Quantification of chemical weathering rates across an actively eroding hillslope. Earth Planet. Sci. Lett. 242 (1–2), 155–169.
- Guo, F., Yost, R.S., 1998. Partitioning soil phosphorus into three discrete pools of differing availability. Soil Sci. 163 (10), 822–833.
- Hahm, W.J., Riebe, C.S., Lukens, C.E., Araki, S., 2014. Bedrock composition regulates mountain ecosystems and landscape evolution. Proc. Natl. Acad. Sci. 111 (9), 3338–3343.
- Harden, J.W., 1987. Soils Developed in Granitic Alluvium Near Merced, California. 1590A.
- Heimsath, A.M., Dietrich, W.E., Nishiizumi, K., Finkel, R.C., 1997. The soil production

- function and landscape equilibrium. Nature 388 (6640), 358-361.
- Hilton, R.G., Galy, A., Hovius, N., 2008. Riverine particulate organic carbon from an active mountain belt: importance of landslides. Glob. Biogeochem. Cycles 22 (1), GB1017.
- Homyak, P.M., Sickman, J.O., Melack, J.M., 2014. Pools, transformations, and sources of P in high-elevation soils: implications for nutrient transfer to Sierra Nevada lakes. Geoderma 217–218, 65–73.
- Hovius, N., Stark, C.P., Allen, P.A., 1997. Sediment flux from a mountain belt derived by landslide mapping. Geology 25 (3), 231–234.
- Hurst, M.D., Mudd, S.M., Walcott, R., Attal, M., Yoo, K., 2012. Using hilltop curvature to derive the spatial distribution of erosion rates. J. Geophys. Res. Earth Surf. 117 (F2) (n/a-n/a).
- Izquierdo, J.E., Houlton, B.Z., van Huysen, T.L., 2013. Evidence for progressive phosphorus limitation over long-term ecosystem development: examination of a biogeochemical paradigm. Plant Soil 367 (1), 135–147.
- Jobbágy, E.G., Jackson, R.B., 2004. The uplift of soil nutrients by plants: biogeochemical consequences across scales. Ecology 85 (9), 2380–2389.
- Johnson, D.L., Watson-Stegner, D., 1987. Evolution model of pedogenesis. Soil Sci. 143 (5), 349–366.
- Kautz, C.Q., Martin, C.E., 2007. Chemical and physical weathering in New Zealand's Southern Alps monitored by bedload sediment major element composition. Appl. Geochem. 22 (8), 1715–1735.
- Korup, O., McSaveney, M.J., Davies, T.R.H., 2004. Sediment generation and delivery from large historic landslides in the Southern Alps, New Zealand. Geomorphology 61 (1–2), 189–207.
- Lajtha, K., Schlesinger, W.H., 1988. The biogeochemistry of phosphorus cycling and phosphorus availability along a desert soil chronosequence. Ecology 69 (1), 24–39.
- Larsen, I.J., Almond, P.C., Eger, A., Stone, J.O., Montgomery, D.R., Malcolm, B., 2014a. Rapid soil production and weathering in the Southern Alps, New Zealand. Science 343 (6171), 637–640.
- Larsen, I.J., Montgomery, D.R., Greenberg, H.M., 2014b. The contribution of mountains to global denudation. Geology 42 (6), 527–530.
- Lebedeva, M.I., Fletcher, R.C., Brantley, S.L., 2010. A mathematical model for steadystate regolith production at constant erosion rate. Earth Surf. Process. Landf. 35 (5), 508–524.
- Little, T.A., Cox, S., Vry, J.K., Batt, G., 2005. Variations in exhumation level and uplift rate along the obliqu-slip Alpine fault, central Southern Alps, New Zealand. Geol. Soc. Am. Bull. 117 (5–6), 707–723.
- Mage, S.M., Porder, S., 2013. Parent material and topography determine soil phosphorus status in the Luquillo Mountains of Puerto Rico. Ecosystems 16 (2), 284–294.
- Marx, S.K., McGowan, H.A., Kamber, B.S., 2009. Long-range dust transport from eastern Australia: a proxy for Holocene aridity and ENSO-type climate variability. Earth Planet. Sci. Lett. 282 (1–4), 167–177.
- McClintock, M.A., Brocard, G., Willenbring, J., Tamayo, C., Porder, S., Pett-Ridge, J.C., 2015. Spatial variability of African dust in soils in a montane tropical landscape in Puerto Rico, Chem. Geol. 412, 69–81.
- Merritts, D.J., Chadwick, O.A., Hendricks, D.M., Brimhall, G.H., Lewis, C.J., 1992. The mass balance of soil evolution on Late Quaternary marine terraces, northern California. Geol. Soc. Am. Bull. 104 (11), 1456–1470.
- Milodowski, D.T., Mudd, S.M., Mitchard, E.T.A., 2014. Erosion rates as a potential bottom-up control of forest structural characteristics in the Sierra Nevada Mountains. Ecology 96 (1), 31–38.
- Milodowski, D.T., Mudd, S.M., Mitchard, E.T.A., 2015. Topographic roughness as a signature of the emergence of bedrock in eroding landscapes. Earth Surf. Dyn. 3 (4), 483–499.
- Mudd, S.M., Yoo, K., 2010. Reservoir theory for studying the geochemical evolution of soils. J. Geophys. Res. Earth 115.
- Murphy, J., Riley, J.P., 1962. A modified single solution method for the determination of phosphate in natural waters. Anal. Chim. Acta 27, 31–36.
- Nelson, D.L., Nelson, D.L., Lehninger, A.L., Cox, M.M., 2008. Lehninger Principles of Biochemistry. W.H. Freeman, New York.
- NIWA, 2016. National Climate Database. New Zealand National Institute of Water and Atmospheric Research.
- Olsen, S.R., Sommers, L.E., 1982. Determination of available phosphorus. In: Page, A.L., Miller, R.H., Keeney, D.R. (Eds.), Method of Soil Analysis. American Society of Agronomy, Madison, WI, pp. 403.
- Paytan, A., McLaughlin, K., 2007. The oceanic phosphorus cycle. Chem. Rev. 107 (2), 563–576.
- Peltzer, D.A., Wardle, D.A., Allison, V.J., Baisden, W.T., Bardgett, R.D., Chadwick, O.A., Condron, L.M., Parfitt, R.L., Porder, S., Richardson, S.J., Turner, B.L., Vitousek, P.M., Walker, J., Walker, L.R., 2010. Understanding ecosystem retrogression. Ecol. Monogr. 80 (4), 509–529.
- Porder, S., Hilley, G., 2011. Linking chronosequences with the rest of the world: predicting soil phosphorus content in denuding landscapes. Biogeochemistry 102 (1), 153–166.
- Porder, S., Ramachandran, S., 2013. The phosphorus concentration of common rocks—a potential driver of ecosystem P status. Plant Soil 367 (1), 41–55.
- Porder, S., Hilley, G.E., Chadwick, O.A., 2007a. Chemical weathering, mass loss, and dust inputs across a climate by time matrix in the Hawaiian Islands. Earth Planet. Sci. Lett. 258 (3–4), 414–427.
- Porder, S., Vitousek, P., Chadwick, O., Chamberlain, C., Hilley, G., 2007b. Uplift, erosion, and phosphorus limitation in terrestrial ecosystems. Ecosystems 10 (1), 159–171.
- R Core Team, 2017. R: A Language and Environment for Statistical Computing. R Foundation for Statistical Computing, Vienna.
- Richardson, S., Peltzer, D., Allen, R., McGlone, M., Parfitt, R., 2004. Rapid development of phosphorus limitation in temperate rainforest along the Franz Josef soil

- chronosequence. Oecologia 139 (2), 267-276.
- Riebe, C.S., Kirchner, J.W., Granger, D.E., Finkel, R.C., 2000. Erosional equilibrium and disequilibrium in the Sierra Nevada, inferred from cosmogenic 26Al and 10Be in alluvial sediment. Geology 28 (9), 803–806.
- Riebe, C.S., Kirchner, J.W., Finkel, R.C., 2003. Long-term rates of chemical weathering and physical erosion from cosmogenic nuclides and geochemical mass balance. Geochim. Cosmochim. Acta 67 (22), 4411–4427.
- Ross, C.W., Mew, G., Searle, P.L., 1977. Soil sequences on two terrace systems in the North Westland area, New Zealand. N. Z. J. Sci. 20, 231–244.
- Saucedo, G.J., Wagner, D.L., 1992. Geologic map of the Chico quadrangle. In: Regional Geologic Map. 7A California Division of Mines and Geology.
- Saunders, W.M.H., Williams, E.G., 1955. Observations on the determination of total organic phosphorus in soils. J. Soil Sci. 6 (2), 254–267.
- Selmants, P.C., Hart, S.C., 2010. Phosphorus and soil development: does the Walker and Syers model apply to semiarid ecosystems? Ecology 91 (2), 474–484.
- Smeck, N.E., 1985. Phosphorus dynamics in soils and landscapes. Geoderma 36 (3), 185–199
- Smith, B.F.L., Bain, B.C., 1982. A sodium hydroxide fusion method for the determination of total phosphate in soils. Commun. Soil Sci. Plant Anal. 13 (3), 185–190.
- Soil Survey Staff, 2014. Keys to Soil Taxonomy, 12 ed. USDA-Natural Resources Conservation Service, Washington, DC.
- Stevens, P.R., 1968. A Chronosequence of Soils Near the Franz Josef Glacier. University of Canterbury, Lincoln (389 pp.).
- Tiessen, H., Moir, J.O., 1993. Characterization of available P by sequential extraction. In: Carter, M.R., Gregorich, E.G. (Eds.), Soil Sampling and Methods of Analysis. Canadian Society of Soil Science.
- Tippett, J.M., Kamp, P.J.J., 1993. Fission track analysis of the Late Cenozoic vertical kinematics of continental pacific crust, South Island, New Zealand. J. Geophys. Res. Solid Earth 98 (B9), 16119–16148.
- Tonkin, P.J., Basher, L.R., 2001. Soil chronosequences in subalpine superhumid Cropp Basin, western Southern Alps, New Zealand. N. Z. J. Geol. Geophys. 44 (1), 37-45.
- Basin, western Southern Alps, New Zealand. N. Z. J. Geophys. 44 (1), 87—45.
 Turner, B.L., Condron, L.M., 2013. Pedogenesis, nutrient dynamics, and ecosystem velopment: the legacy of TW Walker and JK Syers. Plant Soil 367 (1–2), 1–10.
- Turner, B., Laliberté, E., 2015. Soil development and nutrient availability along a 2 million-year coastal dune chronosequence under species-rich Mediterranean shrubland in southwestern Australia. Ecosystems 18 (2), 287–309.
- Uhlig, D., von Blanckenburg, F., 2016. Deep Subsoil Tree Phosphorus Sources in Forest

- Ecosystems, Goldschmidt 2016. European Association of Geochemistry and Geochemical Society, Yokohama.
- Vitousek, P.M., 2004. Nutrient cycling and limitation. In: Princeton Environmental Institute Series Princeton University Press, Princeton.
- Vitousek, P., Chadwick, O., Matson, P., Allison, S., Derry, L., Kettley, L., Luers, A., Mecking, E., Monastra, V., Porder, S., 2003. Erosion and the rejuvenation of weathering-derived nutrient supply in an old tropical landscape. Ecosystems 6 (8), 762–772
- Wakabayashi, J., Sawyer, T.L., 2001. Stream incision, tectonics, uplift, and evolution of topography of the Sierra Nevada, California. J. Geol. 109 (5), 539–562.
- Walker, T.W., Syers, J.K., 1976. The fate of phosphorus during pedogenesis. Geoderma 15 (1), 1–19.
- Wang, X., Yoo, K., Mudd, S.M., Weinman, B., Gutknecht, J., Gabet, E.J., 2018. Storage and export of soil carbon and mineral surface area along an erosional gradient in the Sierra Nevada, California. Geoderma 321, 151–163.
- Wardle, P., 1977. Plant communities of Westland National Park (New Zealand) and neighbouring lowland and coastal areas. N. Z. J. Bot. 15 (2), 323–398.
- Wells, A., Goff, J., 2007. Coastal dunes in Westland, New Zealand, provide a record of paleoseismic activity on the Alpine fault. Geology 35 (8), 731–734.
- Whitehouse, I.E., 1988. Geomorphology of the central Southern Alps, New Zealand: the interaction of plate collision and atmospheric circulation. Z. Geomorph. N.F. Suppl. 69, 105–116.
- Yang, X., Post, W.M., 2011. Phosphorus transformations as a function of pedogenesis: a synthesis of soil phosphorus data using Hedley fractionation method. Biogeosciences 8 (10), 2907–2916.
- Yoo, K., Mudd, S.M., 2008. Discrepancy between mineral residence time and soil age: implications for the interpretation of chemical weathering rates. Geology 36 (1), 35–38.
- Yoo, K., Weinman, B., Mudd, S.M., Hurst, M., Attal, M., Maher, K., 2011. Evolution of hillslope soils: the geomorphic theater and the geochemical play. Appl. Geochem. 26 (Supplement), S149–S153.
- Yoo, K., Fisher, B., Ji, J.L., Aufdenkampe, A., Klaminder, J., 2015. The geochemical transformation of soils by agriculture and its dependence on soil erosion: an application of the geochemical mass balance approach. Sci. Total Environ. 521, 326–335.
- Zemunik, G., Turner, B.L., Lambers, H., Laliberté, E., 2015. Diversity of plant nutrient-acquisition strategies increases during long-term ecosystem development. Nat. Plants 1, 15050.